

**The Potential for Using Geomagnetic Data
in Ocean and Climate Studies.**

**I: Theory of Electromagnetic Fields
Induced by Ocean Currents.**

**Robert H. Tyler and Lawrence A. Mysak
C²GCR Report No. 93-20
December 1993**

The Potential for Using Geomagnetic Data
in Ocean and Climate Studies. I: Theory of
Electromagnetic Fields induced by Ocean
Currents.

Robert H. Tyler and Lawrence A. Mysak

December 1993

Department of Atmospheric and Oceanic Sciences
and
Centre for Climate and Global Change Research
McGill University
805 Sherbrooke St. W.
Montréal, Québec

Abstract

Ocean currents induce magnetic fields. The transport of heat by ocean currents is an important factor in determining the climate of certain regions. Correlations that have been observed between variations in climatic and magnetic records may be explained by noting that changes in ocean circulation could effect changes in both the observed magnetic field and climate of a region.

In a series of *C²GCR* reports, we will investigate the potential for using geomagnetic records in climate studies. The geomagnetic record may be superior in many ways to other records for indicating past and present climate. In later reports we will numerically model the magnetic field induced by global ocean currents. In this report we will present the theory involved and seek analytic solutions of idealized boundary-value problems that will help us understand the physical processes of magnetic induction in the ocean. In this report we will work strictly in an inertial reference frame for which Special Relativity applies. In the next report we will present equations appropriate for a rotating (accelerating) system for which General Relativity should be used.

After scaling the electromagnetic equations, a simple governing “induction” equation is derived in which the conductivity varies spatially. Further scaling can be introduced with respect to the oceanic variables. We find that the ocean currents can induce magnetic fields of up to hundreds (and in some cases perhaps even thousands) of nanoteslas. These magnetic fields are not confined to the ocean and may decay only slightly over large distances so as to remain measurable at locations on land.

Induction in the ocean depends significantly on the magnitudes and gradients of the vertical component of the earth’s field, the conductivity, the oceanic mass transport, and the bathymetry and baroclinicity of the flow.

The characteristic of barotropic flow is to create electrical currents in the horizontal plane leading to a secondary vertical magnetic field component. The baroclinic component of the flow is at least as important and can generate magnetic fields in the horizontal plane that ‘leak’ out of the ocean in some areas and are drawn back in others. This leakage may be largest where there are strong gradients in either the ocean depth or the baroclinicity of the flow.

Contents

1	Theories Relating Climate and Magnetism	1
2	Motivation	4
3	Equations	7
3.1	Primitive Equations	9
3.2	Scaling the Primitive Equations	11
3.3	Approximate System of Equations	12
3.4	Governing Equation for Magnetic Field \mathbf{B}	13
4	Analytic Solutions	15
4.1	Ocean Surface Currents	16
4.2	Ocean Surface Currents including Horizontal Shear	19
4.3	Baroclinic Ocean Currents over an Insulating Seafloor	21
4.4	Induction of the Vertical Magnetic Component	23
5	Other Relationships	24
5.1	Importance of Bathymetry and Baroclinicity	27
5.2	Importance of Variations in Conductivity and the Vertical Component of the Earth's Magnetic Field F_z	32
5.3	Leakage of Magnetic Field out of the Ocean	33
5.4	When Vertical Motions are Important	35
6	Discussion	36
7	Appendix	37
8	Acknowledgements	39
9	References	40

List of Symbols

B magnetic induction (T)

H magnetic field intensity (A/m)

J electric current volume density (A/m^2)

D displacement vector (C/m^2)

ρ_e electric charge density (C/m^3)

E electric field (V/m)

$\mu_o = 4\pi \times 10^{-7}$ H/m magnetic permeability of free space

$\epsilon = \epsilon_r \epsilon_o$ absolute electric permittivity (F/m)

$\epsilon_o = 8.854 \times 10^{-12}$ electric permittivity of free space

$\epsilon_r \approx 80$ relative permittivity (dimensionless)

σ electric conductivity (S/m)

$\gamma_r = (1 - u^2/c^2)^{-1/2} \approx 1$ relativistic factor

$c = (\mu_o \epsilon_o)^{-1/2}$ speed of light $\approx 3 \times 10^8$ m/s

$K = (\sigma \mu_o)^{-1}$ magnetic diffusivity (m^2/s)

$\Omega = 2\pi/1 \text{ day} \approx 7.3 \times 10^{-5}$ radians/s rotation rate of the earth

$R_E \approx 6370$ km, radius of earth

D_t total derivative (time rate of change moving with the fluid)

$\mathbf{u} = u\hat{x} + v\hat{y} + w\hat{z}$ velocity of ocean currents

ϕ latitude

ϕ_o reference latitude

$\vec{\phi}_l$ magnetic flux (magnetic field integrated through depth of ocean)

u_o ocean velocity at surface

μ depth decay factor of flow

F magnetic field (magnetic induction) of earth

b secondary magnetic field due to ocean induction

γ depth decay factor of conductivity

Q electric current strength per unit length

I electric current

λ horizontal wave number of ocean current shear

$$\beta = (\gamma^2 + 4\lambda^2)^{1/2}$$

$\tau_m = \mathcal{L}^2/K$ time scale of magnetic diffusion

$\tau_c = \mathcal{L}/U$ time scale of advection by ocean currents

Units

S = siemens = A/V

Wb = webers = V · s

H = henries = Wb/A

$F = \text{farads} = C/V$

$C = \text{coulombs}$

$A = \text{amperes} = C/s$

$T = \text{teslas} = \text{Wb}/m^2$

$V = \text{volts}$

$s = \text{seconds}$

$m = \text{meters}$

List of Scaling Parameters

\mathcal{L} Horizontal scale $\approx 100 \text{ km}$

\mathcal{D} depth scale of wind-driven ocean current $\approx 100 \text{ m}$

\mathcal{H} water depth $\approx 5000 \text{ m}$

\mathcal{E} magnitude of electric field

$\mathcal{B} = b + \mathcal{F}$

\mathcal{F} magnitude of earth's magnetic field $\approx 3 \times 10^{-5} - 6 \times 10^{-5} \text{ T}$

b magnitude of magnetic field induced by ocean $b \approx 10^{-7} \text{ T} \ll \mathcal{F}$

\mathcal{T} typical time scale for large-scale electric adjustment in ocean $\approx \tau_m \approx 1 \text{ day}$

\mathcal{U} magnitude of horizontal ocean currents $\approx 0.1 - 1 \text{ m/s}$ (intense boundary currents)

\mathcal{W} magnitude of vertical ocean currents $\ll .1 \text{ m/s}$

$\alpha = \mathcal{D}/\mathcal{L} \approx 10^{-3}$ vertical aspect ratios

$\alpha_w = \mathcal{W}/\mathcal{U} \ll 10^{-1}$ ratio of vertical to horizontal ocean velocities

$\alpha_m = b/\mathcal{B} \approx 10^{-3}$ ratio of ocean-induced to total magnetic fields

$R_{m,c} = \frac{u\mathcal{L}}{K} \approx 10^{-1} \rightarrow 1$ magnetic Reynolds number for horizontal flow

List of Figures

1	ENSO and magnetic activity	44
2	Electrical conductivity as a function of salinity and temperature .	44
3	Electrical conductivity of the global ocean	44
4	Induction by ocean surface current	44
5	Ocean surface velocity with horizontal shear	44
6	Induction by ocean surface currents including horizontal shear . .	45
7	Electrical field E_y and current density J_y	45
8	Ocean surface currents over insulating ocean bottom	45
9	Baroclinic mode over insulating ocean bottom	45
10	Double ocean gyre	45
11	Induction by large-scale ocean gyres	46
12	Solution when all charge recirculates at depth	46
13	Dependence of magnetic profile on D/H	46
14	Leakage of magnetic field out of ocean	46

1 Theories Relating Climate and Magnetism

A number of articles have been published attempting to relate variations in the earth's magnetic field to climate variations. While some investigations (to be discussed next) involve seeking mechanisms to relate the magnetic field to the atmospheric pressure, temperature or wind fields, other diverse studies propose, for example, relationships between the magnetic field and the earth's orbital eccentricity (e.g., Wollin *et al.* 1977), or between the magnetic field, climate, volcanic activity and faunal extinctions (Kennett and Watkins, 1970). However, there are few articles presenting compelling causal mechanisms relating magnetic variations to climate. Most of these mechanisms are described only qualitatively and invoke variations in the stream of corpuscular radiations from the Sun.

Bucha (1980, 1988, 1991) assumes that the geomagnetic activity can be used as an indicator of the amount of corpuscular radiation reaching the earth and proposes that variations in this radiation, although energetically small, can alter temperature and pressure patterns over the poles which trigger changes in the general circulation of the atmosphere.

In a more specific account (Bucha, 1988), these circulation changes are presumed to be brought about by changes in the heat balance of the troposphere. The changes in heat balance are caused by a chain of events starting with variations in the relativistic electron precipitation from the outer radiation belts of the earth into the mesosphere and stratosphere. Increases in charged-particle radiation and bremsstrahlung initiate the formation of cirrus clouds and thus change the heat balance of the troposphere.

Since the descending flux of the corpuscular radiation is expected to peak in the auroral ovals (centered on the geomagnetic poles), changes in the position of the geomagnetic poles are used to explain climate fluctuations on longer time scales.

Wollin *et al.* (1981) propose two possible mechanisms. In the first, an increase

in the Sun's magnetism leads to an increase in corpuscular radiation reaching the earth's stratosphere. This leads to an increase in the formation of nitrogen oxides, and increased absorption of direct solar radiation. The increased absorption is followed by an increase in ozone concentrations in the stratosphere which leads to a decrease in surface air temperatures.

In the second mechanism Wollin *et al.* suggest that the variations in the Sun's magnetic field and corpuscular radiation may influence the electrical conductivity and potential of the earth's ionosphere. Changes in the electrical properties (and electromagnetic forcing) in the ionosphere would change the circulation in the ionosphere which could in turn alter circulation of the lower atmosphere and oceans.

A few other mechanisms also relying on corpuscular radiation variations are reviewed in Wollin *et al.* (1981).

Here we propose a mechanism whereby geomagnetism and climate may be related in a way that does not directly involve the Sun. The mechanism is quite simple. Ocean currents generate magnetic fields (Longuet-Higgins *et al.*, 1954; Sanford, 1971). Also, in transporting heat and moisture, the ocean currents help to establish different climate regimes on local and global scales. Thus, since ocean currents both generate magnetic fields and control climate, it is easy to see how magnetic fields and climate may be related.

But there are some complications. Most of the vast collections of geomagnetic data have been taken at observatories on land, by airplanes, or by satellites at an altitude of several hundred kilometers. Few data have been taken within the ocean.

Simple analytic solutions have been presented for the magnetic fields generated by the oceans. These solutions as well as solutions drawn from analogies with electric circuits usually consist of magnetic fields that, while substantial within the water, cancel outside of the water. In a series of *C²GCR* reports we

intend to show that ocean currents induce measurable magnetic fields that reach out of the water and are of large scale, perhaps even reaching inland locations thousands of kilometers away.

In addition to the early and widely cited papers of Longuet-Higgins *et al.* (1954) and Sanford (1971), a number of other papers have appeared describing theories and observations which relate the electric and electric potential fields to the ocean volume (or, in some cases, conductivity) transport (Sanford, 1982; Sanford and Flick, 1974; Larsen 1992; Lilley *et al.* (1986); Chave and Luther, 1990; Luther *et al.* (1991)). Considerable effort has been directed toward trying to use voltage measurements across submerged cables to describe the transport of the Florida current (Sanford, 1982; Larsen 1992; Larsen and Sanford (1985)). Also, a method of using the difference in measurements between electrodes towed behind ships has been developed to indicate the ocean surface flow (for a thorough description of this method and other relevant instrumentation see Filloux, 1987).

Very recently, a study has been published relating changes in ocean-bottom electric and magnetic measurements to the passage of a large- scale ocean eddy (Lilley, 1993). The magnetic fields generated are found to have a maximum strength of 226 nanoteslas, and the form of the field is similar to that which would be expected from the results presented here using a different method of calculation that will be discussed below.

Most of the work on motionally-induced electromagnetic fields in the sea involve integration of equations for the induced electric fields. By contrast, in this report we follow developments in the field of magnetohydrodynamics (MHD), and seek solutions to a governing “induction” differential equation. The advantages of this approach were pointed out early on by Weaver (1965) who calculated the magnetic fields induced by ocean waves and swell; similar methods were used to analyze induction by internal waves (Beal and Weaver, 1970).

2 Motivation

The establishment of the influence of ocean currents on magnetic observations would be quite important. A first attempt at numerically modeling the magnetic induction by the global oceanic circulation has been recently performed by Stephenson and Bryan (1992). As will be discussed in more detail in a forthcoming *C²GCR* report, this study only used a two-dimensional barotropic ocean current field. We will present evidence in this report and in numerical results to follow that the baroclinic modes are often more efficient than the barotropic modes in inducing magnetic fields. Hence realistic solutions of the global ocean induction should involve a three-dimensional description of the velocity and conductivity.

Investigators studying magnetic fields due to inner-earth processes usually treat induction by the ocean as noise (Robert Langel 1993, pers. comm.). In such studies it would be useful to separate out any systematic effects due to the ocean currents.

The geomagnetic records may also contain a wealth of new information about the oceans and climate. The geomagnetic data set is in many ways superior to the climate data set. We shall now try to explain why this is the case.

A collection of permanent observatories around the globe (together with some concepts of the way the magnetic field should behave) has afforded reconstructions of the evolution of the earth's global magnetic field during the past hundred years (for example, see Bloxham and Jackson, 1992). Similar detailed spatial pictures showing global temperature evolution are not available. More specifically, magnetic fields must be nondivergent. Also, in as much as air can be treated as an insulator, the magnetic fields recorded above the lands and ocean will also be irrotational. This allows us to infer much about the geomagnetic field in places where we have no data. In contrast, the air temperature field, for example, is not as easily constrained. We usually have the case that if we do not have temperature

data from a certain region in the ocean or atmosphere, then we simply do not know the temperature in that region—hence the difficulty in creating an evolving picture of global historical temperatures.

Currently, hundreds of permanent and repeat stations around the globe provide high-frequency digital magnetic data in a rather standard format. Interestingly enough, in some regions like the Arctic where there has been historically a paucity of conventional ocean and climate observations, the coverage of magnetic observations has been rather good. In recent years, satellite and airborne observations have provided exceptional global coverage of the earth's magnetic field and its variations.

Perhaps most importantly, magnetic field observations might allow us to see features of ocean circulation that would otherwise be difficult or impossible to detect. Here are two examples.

First, observations of ocean currents usually involve instruments directly measuring the current velocities, or they measure the pressure field and large-scale flow patterns are inferred from this. Because of the variability within the ocean a great number of such observations is usually required. Ocean-induced magnetic fields, on the other hand, may be measured more conveniently (perhaps at land observatories) and also, the electromagnetic signals probably represent an integrated effect of the large-scale ocean currents (Sanford, 1982). Sanford (1982) has also pointed out that the electromagnetic signals describe heat transport by ocean currents (since electrical conductivity depends on the temperature of the water).

Second, steady magnetic fields will probably pass through sea ice undeformed. In other words, existing magnetic data from satellite observation over the polar regions might contain the only full coverage of ocean circulation ever taken in these regions.

However, if the 'long reach' of these magnetic fields is useful in some regards, it also poses a problem. How can we know that measured magnetic variations are

due to variations in the ocean induction and not due to variations in inductive regions in the ionosphere or earth's core? This is a difficult problem, but there may be some ways to resolve it. Variations in ocean circulation or conductivity are probably quite sluggish compared to the rapid magnetic storms and other variations due to processes in the highly conductive ionosphere. Processes at the earth's core might involve all frequencies. However, the geometric filtering and electromagnetic filtering by the mantle are thought to prevent all but the lowest frequencies from reaching the earth's surface. Hence, it is thought that at the earth's surface, magnetic fields due to the earth's core can only appear as relatively smooth, slowly-varying fields with periods of tens of years and longer. Hence, there may be a fortuitous 'spectral window' through which we can view interannual variations in say the ocean-induced fields.

One of the strongest interannual signals in the atmosphere/ocean system is that of ENSO (El Niño/Southern Oscillation). During ENSO events there are anomalies in ocean circulation and electrical conductivity along the Equatorial Pacific.

In a recent article, Bucha (1993; together with the ideas presented in earlier articles) asserts that ENSO events are modulated by changes in corpuscular radiation reaching the polar regions. These changes lead to an alternation between the basic meridional and zonal types of atmospheric circulation. During events of high corpuscular radiation (indicated by increases in the *aa* magnetic activity indices) pressure rises over the Indonesian and North Pacific region. This leads, presumably, to anomalous westerly winds in the western equatorial Pacific. According to Bucha, as the geomagnetic activity decreases, the Aleutian Low deepens and descends to lower latitudes and an equatorial Kelvin wave is formed propagating eastward to the South American coast.

Over the period 1960-1990, Bucha claims that El Niño (indicated by anomalous warmings in the Pacific) as well as the global temperature are significantly

lag-correlated with the geomagnetic activity series. El Niño and the global temperature follow the magnetic activity with a lag of 1.5 and 2.5 years respectively.

Alternatively, we can propose that if magnetic fields measured out of the water are significantly dependent on ocean currents (we will be considering this point later in the report), then we should expect that changes in the ocean currents during ENSO events should be accompanied by changes in the magnetic activity. We will treat data analyses in later *C²GCR* reports. For motivation, however, we note a quick example: In figure 1 we show that ENSO years indeed appear to be associated with peaks in magnetic activity in the region of expected changes in ocean circulation. Except for in the 1980's, there does not appear, however, to be a systematic lag with El Niño following magnetic activity as reported by Bucha. In fact, the strong magnetic peak of the late fifties follows an earlier strong El Niño.

In the remainder of this report we will attempt to develop insight into the processes of electromagnetic induction by ocean currents. Later reports will involve data analyses and numerical models of more realistic ocean current and conductivity configurations.

3 Equations

What we call 'salt' in the ocean is largely a collection of dissociated ions. Sodium chloride—or Na^+ and Cl^- as they appear—are the major constituents. They are relatively difficult to isolate, however, and other constituents such as bromine are also included in modern measurements of 'salinity'.

The dissociated ion together with its hydration sheath has a net charge and as it moves (by being advected by ocean currents) through the earth's magnetic field \mathbf{F} it is subject to a Lorentz force $\mathbf{u} \times \mathbf{B}$ tending to separate the ions in a

line perpendicular to the flow. At high latitudes in the Northern Hemisphere, for example, where \mathbf{F} is essentially downward, positive ions would tend toward the left of the flow while negative ions move to the right. The existence of this ion separation phenomenon in the ocean is well known and most modern current meters in one way or another rely upon it.

As the ions become separated transversely to the flow, a few counter effects may arise. First, the separated ions will induce an electric field that would tend to block further ion separation. Second, the charge might ‘short-circuit’, returning through deeper ocean layers where the ocean velocities (and Lorentz forces) are weaker or have vanished. (In these studies, the air is essentially an insulator.) Third, if the ocean currents extend to depths close to the ocean bottom, charges may short-circuit in the horizontal plane, creating ‘field-aligned currents’ rather than (or in addition to) returning through the deeper water below. Also, on a global scale, there are probably electrical currents that do not short-circuit at all but simply flow along the earth’s circumference. Since electric currents are induced we can expect secondary magnetic fields to arise.

We should mention that a great deal of insight into this topic is afforded through results developed in magnetohydrodynamics (MHD). Most notable is the advantage of working with a governing ‘induction’ equation for the magnetic field rather than integral equations involving the electric current. Also, other MHD results such as Alfvén’s frozen-flux theorem provide insight into induction in the ocean.

Fortunately, the problem of induction by ocean currents is much simpler than the general MHD problem. In the ocean the electrodynamic forces will exert a negligible body force on the fluid and hence the ocean velocities can be prescribed in advance. This is in contrast to the case of a plasma where the flow of the highly ionized fluid is largely dependent on the ensuing electrodynamic forces and the fluid velocities must be solved for simultaneously with the electromagnetic variables.

3.1 Primitive Equations

At the core of any quantitative approach to these ideas are Maxwell's equations. We also will make use of some constitutive relationships describing the properties of the materials, and Ohm's Law which here is a parameterization of the drift of charge subject to an electric field, molecular collisions and advection by ocean currents. These equations are described below.

Maxwell's Equations

The following is a list of Maxwell's equations. For an insightful description of these see Lorrain *et al.* (1988). In the Amperian formulation we have:

$$\nabla \cdot \mathbf{B} = 0 \quad (1)$$

$$\nabla \times \mathbf{B} = \frac{1}{\mu_0} \mathbf{J}_{\text{total}} + \frac{1}{c^2} \partial_t \mathbf{D} \quad (2)$$

$$\nabla \cdot \mathbf{E} = \rho_{\text{total}} / \epsilon_0 \quad (3)$$

$$\nabla \times \mathbf{E} = -\partial_t \mathbf{B} \quad (4)$$

where

$$\rho_{\text{total}} = \rho_e - \nabla \cdot \mathbf{P}, \quad (5)$$

$$\mathbf{J}_{\text{total}} = \mathbf{J} + \partial_t \mathbf{P} + \nabla \times \mathbf{M}, \quad (6)$$

and \mathbf{M} is the magnetization (A/m).

In the presence of a dielectric material the following Minkowskian formulation of Maxwell's equations is useful.

$$\nabla \cdot \mathbf{B} = 0 \quad (7)$$

$$\nabla \times \mathbf{H} = \mathbf{J} + \partial_t \mathbf{D} \quad (8)$$

$$\nabla \cdot \mathbf{D} = \rho_e \quad (9)$$

$$\nabla \times \mathbf{E} = -\partial_t \mathbf{B} \quad (10)$$

Constitutive Relationships

We assume that the electric properties of the media are linear and isotropic and that the magnetic susceptibility is zero. Then we can write

$$\mathbf{H} = \mathbf{B}/\mu_o, \quad (11)$$

$$\mathbf{D} = \epsilon\mathbf{E}. \quad (12)$$

Here, μ_o is the permeability of free space and

$$\epsilon = \epsilon_r \epsilon_o$$

is the absolute permittivity. ϵ_r is the relative permittivity which in the case of sea water is quite large (see *List of Symbols*). This will be especially important in determining the amount of space charges set up by ocean currents.

Ohm's Law

$$\mathbf{J} = \sigma\mathbf{E}' + \rho_e\mathbf{u} \quad (13)$$

Here we take $\sigma = \sigma(x, y, z, t)$ to be a real scalar field, representing a medium with variable but isotropic conductivity. The term $\rho_e\mathbf{u}$ represents electrical currents due to charge advection, and \mathbf{E}' is the electric field measured in a frame of reference moving with the fluid at velocity \mathbf{u} .

Lorentz Transformation

The fields \mathbf{E} and \mathbf{B} depend on the reference frame in which they are measured. This is especially relevant since geophysical records are generally taken on or with respect to a rotating earth. Also, as is apparent in 13, ions will respond to the electric field observed in a reference frame moving with the ocean currents.

In the moving reference frame we have (with reference to the relatively stationary system)

$$\mathbf{E}' = (1 - \gamma_r)\frac{\mathbf{u} \cdot \mathbf{E}}{u^2}\mathbf{u} + \gamma_r(\mathbf{E} + \mathbf{u} \times \mathbf{B}) \quad (14)$$

$$\mathbf{B}' = (1 - \gamma_r) \frac{\mathbf{u} \cdot \mathbf{B}}{u^2} \mathbf{u} + \gamma_r (\mathbf{B} - \mu_o \mathbf{u} \times \mathbf{D}) \quad (15)$$

where γ_r is the relativistic factor

$$\gamma_r = \left(1 - \frac{u^2}{c^2}\right)^{-1/2},$$

with c the speed of light. We are clearly considering nonrelativistic fluid velocities and from here on we take

$$\gamma_r = 1. \quad (16)$$

Further discussion of the equations presented in this section can be found in Gubbins and Roberts (1987).

3.2 Scaling the Primitive Equations

We will scale the primitive equations using the values described in the *List of Scaling Parameters*. We can use many of the same scaling arguments that are used, for example, in the study of magnetohydrodynamics of the earth's core, and the reader is referred to Gubbins and Roberts (1987) for a more detailed description.

We let

$$\begin{aligned} |\nabla \times \mathbf{E}| &\approx \frac{\mathcal{E}}{\mathcal{L}}, \\ |\partial_t \mathbf{B}| &\approx \frac{\mathcal{B}}{\mathcal{T}}. \end{aligned}$$

Then by 10

$$\mathcal{E} \approx \frac{\mathcal{L}}{\mathcal{T}} \mathcal{B}.$$

Then using this result together with 11 and 12 in 8 we see that the ratio of the last term on the right hand side to the term on the left hand side is

$$\frac{|\partial_t \mathbf{D}|}{|\nabla \times \mathbf{H}|} \approx \mu_o \epsilon (\mathcal{L}/\mathcal{T})^2 = \epsilon_r \left[\frac{\mathcal{L}/\mathcal{T}}{c} \right]^2 \ll 1.$$

Hence, for all of our purposes the displacement current $\partial_t \mathbf{D}$ in 8 is negligible.

In a similar manner, we can show that the term involving the displacement \mathbf{D} in 15 is negligible. Hence, for the non-relativistic transformation between moving (primed quantities) and stationary systems we have (to order $(\frac{\mathcal{U}}{c})^2$)

$$\mathbf{E}' = \mathbf{E} + \mathbf{u} \times \mathbf{B} \quad (17)$$

and

$$\mathbf{B}' = \mathbf{B}. \quad (18)$$

Also, to order $\epsilon_r(\mathcal{U}/c)^2$, we can neglect the term representing advection of charge $\rho_e \mathbf{u}$ in 13. This can be seen by comparing $\rho u \approx \epsilon \frac{\mathcal{E}\mathcal{U}}{\mathcal{L}} \approx \epsilon_r \epsilon_o \frac{\mathcal{U}\mathcal{B}}{\mathcal{T}}$ to $\mathbf{J} \approx \frac{1}{\mu_o} \frac{\mathcal{B}}{\mathcal{L}}$, and noting $c = (\mu_o \epsilon_o)^{-1/2}$

3.3 Approximate System of Equations

We have seen that for oceanic induction, where $\mathcal{U}^2 \ll c^2$, the displacement current is negligible, as is the advection of charge compared to \mathbf{J} and the displacement term in 15. We can write the following set of equations using 8 in 13 together with 16 and 17 and 18.

$$\nabla \times \mathbf{B} = \mu_o \mathbf{J} \quad (19)$$

$$\nabla \cdot \mathbf{B} = 0 \quad (20)$$

$$\nabla \cdot \epsilon \mathbf{E} = \rho_e \quad (21)$$

$$\nabla \times \mathbf{E} = -\partial_t \mathbf{B} \quad (22)$$

$$\mathbf{J} = \sigma(\mathbf{E} + \mathbf{u} \times \mathbf{B}). \quad (23)$$

3.4 Governing Equation for Magnetic Field \mathbf{B}

We wish to obtain a governing equation for \mathbf{B} with σ and \mathbf{u} as specified functions. Note that we are not treating the conductivity as a constant. There are two reasons for this. First, we believe that in terms of ocean induction, variations in conductivity will be as important as the variations in the ocean current. To support this assertion we include figures 2 and 3.

In figure 2 we show the ocean's conductivity as a function of temperature and salinity. In figure 3 a map of the ocean surface conductivity is shown. We see that even within the surface layer the conductivity variations are as great as those of the ocean currents. Since we expect that the induced magnetic fields will depend on the product $\sigma\mathbf{u}$, variations of both should be considered. The variations of conductivity with depth will be even more important. The conductivity varies by a factor of about two between the warm surface and colder deep water.

The second reason for including variations in conductivity is that in including conductivity gradients we can avoid having to impose electric flow conditions at the interface between water and air, and water and land. This will be advantageous in the numerical solutions presented in later reports.

From $\nabla \times (19)$, the vector identity

$$\nabla \times \nabla \times \mathbf{B} = \nabla(\nabla \cdot \mathbf{B}) - \nabla^2 \mathbf{B}, \quad (24)$$

and 20, we obtain

$$\mu_o \nabla \times \mathbf{J} = -\nabla^2 \mathbf{B}. \quad (25)$$

Now use 25, 22, and 23 in $\nabla \times (23)$ to yield

$$\partial_t \mathbf{B} - \nabla \times (\mathbf{u} \times \mathbf{B}) - \frac{1}{\sigma \mu_o} \nabla^2 \mathbf{B} - \frac{1}{\sigma \mu_o} \nabla \ln \sigma \times (\nabla \times \mathbf{B}) = 0. \quad (26)$$

When conductivity is constant, the last term in equation 26 vanishes and 26 agrees with a similar equation given in Gubbins and Roberts (1987).

Using the vector identity

$$\nabla \times (\mathbf{u} \times \mathbf{B}) = (\nabla \cdot \mathbf{B})\mathbf{u} - (\nabla \cdot \mathbf{u})\mathbf{B} + (\mathbf{B} \cdot \nabla)\mathbf{u} - (\mathbf{u} \cdot \nabla)\mathbf{B}, \quad (27)$$

noting 20 and assuming the fluid is incompressible ($\nabla \cdot \mathbf{u} = 0$), we can write 26 as

$$D_t \mathbf{B} = (\mathbf{B} \cdot \nabla) \mathbf{u} + K \nabla^2 \mathbf{B} + K \nabla \ln \sigma \times (\nabla \times \mathbf{B}) \quad (28)$$

where $D_t \mathbf{B} = \partial_t \mathbf{B} + \mathbf{u} \cdot \nabla \mathbf{B}$ is the time derivative observed while moving with the fluid at velocity \mathbf{u} .

We can interpret the terms on the right hand side of 28 as follows. The first term can be thought of as representing deformation (stretching and tilting) of the magnetic field lines by the flow \mathbf{u} . The second term represents electromagnetic diffusion, where $K = (\sigma \mu_o)^{-1}$ is the magnetic diffusion coefficient.

We now elaborate on the last term. Since $\nabla \times \mathbf{B}$ is proportional to the electric current density (by equation 19) we see that this term describes variations in the magnetic field due to preferred paths for electric current flow.

We can illustrate this by considering a large tub of water through which we pass a uniform electric current. If the conductivity of the water was originally uniform, then we would expect that the induced magnetic fields at the center of the tub should not vary much horizontally. If now, we heated up one side of the tub—say to one side of the electric current vector—thereby increasing the conductivity, we would expect that the originally uniform current would tend to prefer a path through the side with higher conductivity. This would lead to variations in the induced magnetic field, that would increase until the magnetic field is distorted enough that its curvature is sufficiently large to make the diffusion term important. This adjustment would essentially be instantaneous for the time scales we are first interested in.

It is extremely important to point out that the governing (induction) equation we have derived is not immediately applicable in a coordinate system rotating with the solid earth. In fact, Special Relativity does not extend to a rotating (accelerating) coordinate system and Maxwell's equations and the constitutive relationships do not necessarily retain their form even in an approximate sense. Before we will attempt to model realistic currents, we will need to make a formal

transformation for the rotating system and then attempt to rederive an induction equation that may include extra terms describing the rotation. For now, the purpose in the remaining part of this report will be to gain simple insight into the physical mechanisms involved. We will do this in a cartesian domain that is not spinning and is subject to a background magnetic field.

For reference, we will expand 28 into three scalar equations:

$$\begin{aligned}
u\partial_x B_x + v\partial_y B_x + w\partial_z B_x &= B_x\partial_x u + B_y\partial_y u + B_z\partial_z u \\
&+ K\partial_x\partial_x B_x + K\partial_y\partial_y B_x + K\partial_z\partial_z B_x \\
&+ K\partial_y \ln \sigma(\partial_x B_y - \partial_y B_x) - K\partial_z \ln \sigma(\partial_z B_x - \partial_x B_z)
\end{aligned} \tag{29}$$

$$\begin{aligned}
u\partial_x B_y + v\partial_y B_y + w\partial_z B_y &= B_x\partial_x v + B_y\partial_y v + B_z\partial_z v \\
&+ K\partial_x\partial_x B_y + K\partial_y\partial_y B_y + K\partial_z\partial_z B_y \\
&+ K\partial_x \ln \sigma(\partial_y B_x - \partial_x B_y) - K\partial_z \ln \sigma(\partial_z B_y - \partial_y B_z)
\end{aligned} \tag{30}$$

$$\begin{aligned}
u\partial_x B_z + v\partial_y B_z + w\partial_z B_z &= B_x\partial_x w + B_y\partial_y w + B_z\partial_z w \\
&+ K\partial_x\partial_x B_z + K\partial_y\partial_y B_z + K\partial_z\partial_z B_z \\
&+ K\partial_x \ln \sigma(\partial_z B_x - \partial_x B_z) - K\partial_y \ln \sigma(\partial_y B_z - \partial_z B_y)
\end{aligned} \tag{31}$$

4 Analytic Solutions

Now we wish to consider some simple analytic solutions to 29-31.

4.1 Ocean Surface Currents

We first consider a uniform infinite-plane ocean current moving through an imposed uniform vertical magnetic field F_z in a non-rotating reference frame. The ocean velocities are assumed to decay exponentially with depth from the surface,

$$\mathbf{u} = u_o e^{\mu z} \hat{x}, \quad z < 0. \quad (32)$$

We also have $v = w = 0$. Since u only varies with z , we expect $\partial_x = \partial_y = 0$. We take the conductivity as uniform in the infinitely-deep water and zero above $z = 0$. Then the magnetic diffusivity $K = (\mu_o \sigma)^{-1}$ is a constant in the water and infinite everywhere else.

Equation 29 then becomes

$$\partial_z \partial_z B_x = -\frac{1}{K} B_z \partial_z u = -\frac{1}{K} F_z \mu u_o e^{\mu z}. \quad (33)$$

In 33 we have replaced B_z with F_z . In general B_z would be the sum of the imposed field F_z plus contributions due to the induction by ocean currents. In the case of the earth, the imposed background field F_z , away from the magnetic equator, will be of order 10^4 nT while induction in the ocean may be of order 100 nT or less. Hence, over most of the globe, $B_z = F_z + b_z \approx F_z$ where b_z represents the contribution by ocean induction. This result is important for later work. For the infinite-plane geometry here, we actually expect that $b_z = 0$; hence 33 is valid regardless of the magnitude of the imposed field F_z .

Physically, in the problem we are considering, we should expect that the Lorentz force $\mathbf{u} \times \mathbf{B}$ on the ions being advected by \mathbf{u} should lead to a uniform horizontally infinite sheet of current moving in the direction \hat{y} (assuming u_o and F_z are positive). When viewed from far above or below $z = 0$, the solution for B_x should look similar to the solution for an infinite current sheet which is

$$B_x \text{ infinite current sheet} = \pm \frac{1}{2} \mu_o Q_y \quad (34)$$

where Q_y is the current strength per unit length and the sign of B_x is opposite on each side of the sheet. Hence, we expect

$$B_x(z \rightarrow \infty) = -B_x(z \rightarrow -\infty) = C \quad (35)$$

where C is a constant.

With 35 and since $u(z > 0) = 0$, a bounded solution to 33 in region $z \geq 0$ can only be

$$B_x = C \quad z \geq 0. \quad (36)$$

Requiring continuity at $z = 0$ and using 36 we can then obtain the constant of integration while integrating 33 in the region $z \leq 0$. The solution is then

$$B_x = \frac{F_z u_o}{\mu K} \begin{cases} \frac{1}{2} - e^{\mu z} & z \leq 0 \\ -\frac{1}{2} & z \geq 0. \end{cases} \quad (37)$$

If we had let the conductivity decay exponentially with depth from the surface, $\sigma = \sigma_o e^{\gamma z}$, the solution would be only slightly different:

$$B_x = \frac{F_z u_o}{(\mu + \gamma)K} \begin{cases} \frac{1}{2} - e^{(\mu + \gamma)z} & z \leq 0 \\ -\frac{1}{2} & z \geq 0. \end{cases} \quad (38)$$

A plot of the function in 37 is shown in figure 4. It is also seen using 19 and 23 that the electric current density $\mathbf{J} = -\sigma F_z u \hat{y}$ and the electric field \mathbf{E} is zero everywhere.

To compare 37 with 34 we obtain, using 19,

$$\mathbf{J} = \frac{1}{\mu_o} \nabla \times \mathbf{B} = \frac{1}{\mu_o} \partial_z B_x \hat{y}. \quad (39)$$

We can integrate 39 over the ocean depth to get an equivalent sheet current of

$$Q_y = \int_{-\infty}^0 J_y dz = \frac{1}{\mu_o} \int_{-\infty}^0 \frac{-F_z u_o}{K} e^{\mu z} dz = \frac{-F_z u_o}{\mu_o K} \frac{1}{\mu}. \quad (40)$$

Using 40 in 37 we can obtain B_x in a form similar to 34. This indicates that in this example of an infinite ocean current, the induced magnetic field when observed above or far below the ocean appears similar to that due to an infinite electric current sheet.

From 40 we see that for typical terrestrial values of $F_z \approx 30 \times 10^3$ nT, $u_o \approx 1$ m/s, $\mu \approx 10^{-2}$ m⁻¹, and $\sigma \approx 5$ S/m, the electric current passing through the ocean would be of order .015 amperes per meter length of the ocean current. If the ocean current were 10^4 km long then the total electric current would be $I = 1.5 \times 10^5$ amperes (small household appliances draw of order 1 ampere). By 37 we see that ocean-induced magnetic field would be of order 15 nT (1.5 nT if we use a more common magnitude of $u_o = .1$ m/s) which, although small, is large enough to be measured.

The calculation above should be viewed with caution regarding its application to the ocean. Aside from the important difference in inertial as opposed to rotating reference frames, the uniform infinite-plane ocean currents allow no charge to return—charge is simply pushed off to infinity. In a realistic case we should expect appreciable electric currents returning through deeper motionless waters. Also, even if the ocean currents were uniform, the conductivity of the water varies considerably, creating ‘preferred’ electric paths (as indicated by the last term in 26). For strong currents extending nearly to the bottom, like the Florida Current and parts of the Antarctic Circumpolar Current, it is conceivable that charge separated along long stretches of the current returns in electric currents concentrated in canyons or other depressions in the bathymetry.

For example, performing a rough calculation similar to the preceding paragraph, but with $\mu = 1$ km⁻¹ and 100 km as the length of the current, typifying the Florida Current, we see that an estimate of the total current would be $I \approx 1.5 \times 10^4$ amperes and the ocean-induced magnetic field \mathbf{b} would be of order 150 nT.

If a similar amount of current returned through confined bathymetric depressions of order 1 km total length (this would have to be a rather narrow submarine canyon, for example), then the electric current would be amplified by a factor of 100 in these areas as would the local \mathbf{b} fields, leading to a magnitude of 15,000 nT, comparable to that of the earth—an interesting result in view of the number

of reported ‘compass failures’ and the more nebulous notoriety of the region.

4.2 Ocean Surface Currents including Horizontal Shear

Consider the ocean current system described in figure 5 which is given by the real part of

$$u = u_o e^{i\lambda y + \mu z} \quad \text{for } z \leq 0, \quad (41)$$

where u_o is the maximum velocity at the surface. Also, we have $v = w = \partial_x = 0$. We take the imposed background magnetic field to be uniform over the domain with components F_y, F_z . We write

$$B_x = b_x, \quad B_y = F_y + b_y \approx F_y, \quad B_z = F_z + b_z \approx F_z$$

where we assume the background main field $F_y, F_z \gg b_y, b_z$.

We consider a conductivity that is zero outside of the water and decays exponentially with depth from the surface. We then have

$$\sigma = \sigma_o e^{\gamma z} \quad \text{for } z \leq 0. \quad (42)$$

The reason for including the depth decay of σ is two-fold. First, since most ocean temperatures cool with depth the conductivity also decreases, with a magnitude about twice as great at the surface as compared to the bottom (*e.g.* Filloux ((1987)). Second, the charge recirculation can be constrained as it would be in the realistic case of a finite depth ocean (the conductivity of the ocean bottom will be much less than that of sea water).

Equation 29 becomes

$$\partial_z \partial_z b_x + \partial_y \partial_y b_x - \partial_z \ln \sigma \partial_z b_x = \frac{1}{K} (-i\lambda F_y - \mu F_z) e^{i\lambda y + \mu z}. \quad (43)$$

We will seek solutions for 43 with a y -dependence of the form $e^{i\lambda y}$ similar to the forcing on the right hand side of 43. Hence, if we use $b_x = Z(z)e^{i\lambda y}$ in 43 and divide through by $e^{i\lambda y}$ we obtain

$$Z'' - \gamma Z' - \lambda^2 Z = -\frac{1}{K}(i\lambda F_y + \mu F_z)u_o e^{\mu z} \quad (44)$$

We can use the appropriate Green's function to solve 44 in the domain $-\infty < z \leq 0$. We first put 44 in a self-adjoint form by multiplying through by $e^{-\gamma z}$ and combining derivatives. This gives

$$\frac{d}{dz}(e^{-\gamma z} \frac{d}{dz} Z) - \lambda^2 e^{-\gamma z} Z = -(i\lambda F_y + \mu F_z) \frac{u_o}{K_o} e^{\mu z} \quad (45)$$

where $K_o^{-1} = \mu_o \sigma(z=0) = \mu_o \sigma_o$.

We must solve 45 subject to two boundary conditions. First, we require

$$Z(z \rightarrow -\infty) = 0 \quad (46)$$

(the ocean can induce no magnetic monopoles). Secondly, in order to have no charge flow across the ocean/air interface we require

$$\mu_o \mathbf{J} \cdot \hat{z} = (\nabla \times \mathbf{B}) \cdot \hat{z} = 0 \quad (47)$$

which, since $\partial_x = 0$ for the geometry of this problem, requires

$$\partial_y B_x(z=0) = -\lambda^2 B_x(z=0) = 0. \quad (48)$$

For non-vanishing λ this can only be satisfied if

$$B_x(z=0) = 0. \quad (49)$$

To solve 45 subject to 46 and 49 we construct the following Green's functions (see appendix B).

$$G(z | \xi) = \frac{1}{\beta} \begin{cases} e^{\frac{\gamma+\beta}{2}z} e^{\frac{\gamma}{2}\xi} \sinh \frac{\beta}{2}\xi & -\infty < z \leq \xi \\ e^{\frac{\gamma}{2}z} \sinh(\frac{\beta}{2}z) e^{\frac{\gamma+\beta}{2}\xi} & \xi \leq z \leq 0 \end{cases} \quad (50)$$

Then, our solution is given by the real part of the expression

$$Z = \int_{-\infty}^0 G(z | \xi) (-i\lambda F_o - \mu F_z) \frac{u_o}{K_o} e^{\mu\xi} d\xi \quad (51)$$

which upon integration gives

$$\begin{aligned} Z(z) = & -(i\lambda F_y + \mu F_z) \frac{u_o}{K_o} \frac{2e^{\frac{\gamma+\beta}{2}z}}{\beta} \left(\frac{1 - e^{(\frac{\gamma+\beta}{2}+\mu)z}}{\gamma + \beta + 2\mu} - \frac{1 - e^{(\frac{\gamma-\beta}{2}+\mu)z}}{\gamma - \beta + 2\mu} \right) \\ & -(i\lambda F_y + \mu F_z) \frac{u_o}{K_o} \frac{2}{\beta} \sinh\left(\frac{\beta}{2}z\right) \left(\frac{1}{\gamma + \beta + 2\mu} e^{(\frac{\gamma+\beta}{2}+\mu)z} \right). \end{aligned} \quad (52)$$

The solution for the induced magnetic field b_x is then

$$\mathbf{b} = b_x \hat{x} = Z e^{i\lambda y} \hat{x}. \quad (53)$$

The contribution from the first term on the right hand side of 53 can be thought of as due to electrical sources above the observation point while the second is due to sources below.

The solution 53 is shown plotted in figure 6. Also, \mathbf{J} and \mathbf{E} are calculated from 19 and 23 and are plotted in figure 7.

We note that this calculation produces a magnetic field that vanishes outside of the water. This is due to the fact that we have assumed that the ocean currents extend to infinity with no along-flow variations. In analogy, we can think of the infinitely-long solenoid which produces a zero-magnetic field outside of the solenoid.

In reality, where the special geometry producing this cancellation of the magnetic field outside of the water does not exist, we should expect that there will be substantial leakage of the magnetic field into the air, with the returning flux showing a new decay scale that is dependent on the finite length (as well as the width) of the ocean current feature.

4.3 Baroclinic Ocean Currents over an Insulating Seafloor

In the last section we assumed the conductivity to decay exponentially with depth. Now we assume that the conductivity is uniform within the water but that the

ocean has a finite depth H with the material below having zero conductivity (in reality, ocean sediment conductivities may reach magnitudes of about a tenth that of the overlying water).

We start by considering a velocity of the form $u = u_o e^{i\lambda y + \mu z}$. The magnetic induction can be calculated in a manner similar to that used in the previous section. The only difference is that in this case the lower boundary condition (at $z = -H$) is similar to the boundary condition at the surface ($b_x = 0$). The details are omitted and the solution for the induced magnetic field is given as follows.

$$b_x = Z e^{i\lambda y} \quad (54)$$

where

$$Z = \frac{(\lambda e^{2\lambda z} + \mu - \mu e^{2\lambda z} + \lambda) (i\lambda F_y + \mu F_z) (u_o/K_o) e^{\mu z - \lambda z}}{(2\lambda + 2\mu) (\lambda - \mu) \lambda (\cosh(\lambda z) - \coth(\lambda(z+H)) \sinh(\lambda z))} \quad (55)$$

$$- \frac{(u_o/K_o) (i\lambda F_y + \mu F_z)}{(\lambda + \mu) (\lambda - \mu) (\cosh(\lambda z) - \coth(\lambda(z+H)) \sinh(\lambda z))}$$

$$- \frac{(\lambda e^{2\lambda z + 2\lambda H} + \mu - \mu e^{2\lambda z + 2\lambda H} + \lambda) (i\lambda F_y + \mu F_z) (u_o/K_o) e^{\mu z - \lambda z - \lambda H}}{(2\lambda + 2\mu) (\lambda - \mu) \lambda (\sinh(\lambda(z+H)) \coth(\lambda z) - \cosh(\lambda(z+H)))}$$

$$+ \frac{(u_o/K_o) (i\lambda F_y + \mu F_z) e^{-\mu H}}{(\lambda + \mu) (\lambda - \mu) (\sinh(\lambda(z+H)) \coth(\lambda z) - \cosh(\lambda(z+H)))}.$$

This solution is shown in figure 8. In (a) we show the velocities over the depth assumed to be $H = -1$ km. In (b) we show the induced magnetic field (calculated from equation 56); in (c), the electric current density J_y (calculated from equations 56 and 19); and in (d), the electric field E_y (calculated from equations 56, 19 and 23).

Instead of an exponential decay of the velocity field, let us now consider a simple baroclinic mode (by letting μ be an imaginary number) such that the surface velocities are equal and opposite to the bottom velocities as shown in figure 9 (a). The induced fields in the order as described in the last example are shown in figure 9 (b)-(c).

We can contrast the induced fields due to surface currents shown in figure 8 with those of the pure baroclinic motion induction shown in figure 9. First notice that the magnetic induction for the baroclinic case (figure 9 (b)) is an order of magnitude larger than that for the surface current case (figure 8 (b)). The reason for this can be described as follows.

In the case of the surface-current profile, charges are separated in the surface layer and drift back in lower layers under the electric field (figure 8 (d)) established by the spatial charges. The motion of these charges is described by the electric current density shown in (figure 8 (c)). In the simple baroclinic mode (figure 9), however, charges are separated in the surface layer and also separated (in an opposite sense) in the lower layers. Hence, even as the charges return below they are forced by a Lorentz force in the direction of their motion.

We see that baroclinic induction is very efficient, at least at producing fields within the ocean. We have a strong practical interest in fields that extend out of the ocean and will return to this point later. We note that for the horizontal flow geometry we have considered here and where the ocean sediments are not conducting, a barotropic mode would produce no magnetic field nor electric currents. Charges would be separated until a spacial charge build-up created an electric field to exactly cancel the Lorentz force. This is in contrast with the baroclinic modes which have no net mass transport yet are quite efficient generators of electric currents and magnetic fields.

4.4 Induction of the Vertical Magnetic Component

Consider an ocean where the conductivity is only a function of depth $\sigma = \sigma(z)$ and vertical velocities are neglected $w = 0$. Equation 31 gives

$$\mathbf{u} \cdot \nabla B_z = K \nabla^2 B_z. \quad (56)$$

Assuming $\nabla^2 F_z = 0$ and also $\nabla F_z \gg \nabla b_z$, we can write

$$\nabla^2 b_z = \frac{1}{K} \mathbf{u} \cdot \nabla F_z. \quad (57)$$

Equation 57 can be solved easily using numerical relaxation schemes. We can, however, also write the solution in closed form using the Green's function for this equation (together with the requirement that $b_z \rightarrow 0$ away from the source areas):

$$G(x, y, z|\xi, \eta, \zeta) = ((x - \xi)^2 + (y - \eta)^2 + (z - \zeta)^2)^{-1/2}$$

(see Butkovskiy, 1982, page 153). The solution for b_z is then

$$b_z = -\frac{1}{4\pi} \int \int \int \frac{\mathbf{u}(\xi, \eta, \zeta) \cdot \nabla F_z(\xi, \eta, \zeta) d\xi d\eta d\zeta}{K((x - \xi)^2 + (y - \eta)^2 + (z - \zeta)^2)^{1/2}}. \quad (58)$$

If the flow is barotropic and the conductivity is constant with depth we can replace 58 by an area integral:

$$b_z = -\frac{1}{4\pi} \int \int \frac{1}{K} \mathbf{u}(\xi, \eta) \cdot \nabla F_z(\xi, \eta, \zeta) \ln \frac{z + H + ((x - \xi)^2 + (y - \eta)^2 + (z + H)^2)^{1/2}}{z + ((x - \xi)^2 + (y - \eta)^2 + z^2)^{1/2}} d\xi d\eta. \quad (59)$$

In calculating the field b_z above the ocean, the integrals in 58 or 59 could be replaced by a summation over all of the source points. This requires, though, that the distance from the sources to the field point being calculated is much greater than the spatial steps used in the summation.

This method is used to calculate the double gyre depth-independent flow shown in figure 10. The field b_z is shown in figure 11.

5 Other Relationships

In deriving the set of equations 29-31 we first scaled the electromagnetic variables. The approximations that followed were quite valid. Other (often weaker) approximations can be made after scaling the oceanographic variables. These extra approximations will allow us to investigate the dominant processes involved in generating magnetic fields by a certain type of prescribed oceanic flow.

If the oceanic flow were isotropic there would be just one length scale of interest. This is not the case however. Advection of the magnetic field occurs on horizontal scales, while magnetic diffusion can act over the much smaller depth

scale as well as the horizontal scales. Hence we will need to account for these differences using coefficients to describe the aspect ratio of these horizontal and vertical scales.

We will start by writing the set of equations 29- 31 in nondimensional form. The coefficients that arise will be the aspect ratios α , α_w , and α_m (see the *List of Scaling Parameters* for a description). Also, we will use the magnetic Reynolds number $R_{m_{\mathcal{L}}}$ derived using the horizontal length scale \mathcal{L} . The magnetic Reynolds number $R_{m_{\mathcal{L}}} = \frac{\mathcal{U}\mathcal{L}}{K}$ is a measure of the relative importance of advection of the magnetic field relative to magnetic diffusion. Another interpretation of $R_{m_{\lambda}}$ can be given upon writing

$$R_{m_{\lambda}} = \tau_m/\tau_c, \quad (60)$$

where

$$\tau_m = \mathcal{L}^2/K, \quad (61)$$

is the time scale for magnetic diffusion (through ohmic resistance) and

$$\tau_c = \mathcal{L}/\mathcal{U} \quad (62)$$

is the time scale for advection of the flow. For many problems we may expect $R_{m_{\lambda}}$ to fall in the range of about 1 to 10.

The procedure for scaling the equations 29-31 will be to let $x \rightarrow \mathcal{L}x$, $y \rightarrow \mathcal{L}y$, $z \rightarrow \mathcal{D}z$, $u \rightarrow \mathcal{U}u$, $v \rightarrow \mathcal{U}v$, $w \rightarrow \mathcal{W}w$, $B_x \rightarrow \mathcal{F}B_x$, $B_y \rightarrow \mathcal{F}B_y$, and $B_z \rightarrow \mathcal{F}B_z$. After some rearrangement of the terms we can write the nondimensional version of 29-31 as

$$\begin{aligned} R_{m_{\mathcal{L}}}[\alpha^2\{u\partial_x B_x + v\partial_y B_x\} + \alpha\{\alpha_w w\partial_z B_x\} + \frac{\alpha^2}{\alpha_m}\{-B_x\partial_x u - B_y\partial_y u\} \\ + \frac{\alpha}{\alpha_m}\{-B_z\partial_z u\}] \\ +[\alpha^2\{-\partial_x\partial_x B_x - \partial_y\partial_y B_x - \partial_y \ln \sigma(\partial_x B_y - \partial_y B_x)\} + \alpha\{-\partial_z \ln \sigma\partial_x B_z\} \\ + \{-\partial_z\partial_z B_x + \partial_z \ln \sigma\partial_z B_x\}] = 0, \quad (63) \end{aligned}$$

$$\begin{aligned}
R_{m_{\mathcal{L}}} \left[\alpha^2 \{u\partial_x B_y + v\partial_y B_y\} + \alpha \{ \alpha_w w \partial_z B_y \} + \frac{\alpha^2}{\alpha_m} \{ -B_x \partial_x v - B_y \partial_y v \} \right. \\
\left. + \frac{\alpha}{\alpha_m} \{ -B_z \partial_z v \} \right] \\
+ [\alpha^2 \{ -\partial_x \partial_x B_y - \partial_y \partial_y B_y - \partial_x \ln \sigma (\partial_y B_x - \partial_x B_y) \}] \\
+ \alpha \{ -\partial_z \ln \sigma \partial_y B_z \} + \{ -\partial_z \partial_z B_y + \partial_z \ln \sigma \partial_z B_y \} = 0, \quad (64)
\end{aligned}$$

$$\begin{aligned}
R_{m_{\mathcal{L}}} [\alpha^2 \{u\partial_x B_z + v\partial_y B_z\} + \alpha \{ \alpha_w w \partial_z B_z \} + \frac{\alpha^2}{\alpha_m} \{ \alpha_w B_x \partial_x w - \alpha_w B_y \partial_y w \}] \\
+ \frac{\alpha}{\alpha_m} \{ -\alpha_w B_z \partial_z w \} \\
+ [\alpha^2 \{ -\partial_x \partial_x B_z - \partial_y \partial_y B_z + \partial_x \ln \sigma \partial_x B_z + \partial_y \ln \sigma \partial_y B_z \}] \\
+ \alpha \{ -\partial_x \ln \sigma \partial_z B_x - \partial_y \ln \sigma \partial_z B_y \} \\
+ \{ -\partial_z \partial_z B_z \} = 0. \quad (65)
\end{aligned}$$

The purpose of writing the equations in nondimensional form is that the magnitude of each of the terms is then contained in the multiplicative coefficients and hence the dominant terms can be identified. We do not change the symbols of the variables but simply note that the variables are nondimensionalized when a nondimensional parameter appears in the equation.

From the values of \mathcal{L} , \mathcal{D} , \mathcal{W} , \mathcal{U} , α etc., listed in the *List of Scaling Parameters*, we see that of the terms multiplied by $R_{m_{\mathcal{L}}}$ in 63 and 64, clearly the $\frac{\alpha}{\alpha_m} \{ \cdot \}$ set dominates over the others. Of the terms not multiplied by $R_{m_{\mathcal{L}}}$, the first order terms will be those with no α multiplier ($\alpha^0 \{ \cdot \}$). For flow where $R_{m_{\mathcal{L}}}$ is close to one, we expect that the leading order terms from each of the bracketed groups will be of comparable magnitude. Then the balances shown in equations 66 and 67 are achieved.

Equation 65 requires more careful consideration. We will primarily be interested in induction by ocean circulation. In this case, if we use as a typical value of w that of typical open-ocean Ekman pumping velocities, *i.e.*, 10^{-8} m/s, we can

show that all of the terms multiplied by $R_{m,c}$ in 65 will be small and we will have the first-order balance given in 68.

$$\partial_z \partial_z B_x - \partial_z \ln \sigma \partial_z B_x = -\frac{\alpha}{\alpha_m} R_{m,c} B_z \partial_z u, \quad (66)$$

$$\partial_z \partial_z B_y - \partial_z \ln \sigma \partial_z B_y = -\frac{\alpha}{\alpha_m} R_{m,c} B_z \partial_z v, \quad (67)$$

$$\partial_z \partial_z B_z = 0. \quad (68)$$

Note that the equations above are of the same form as the one we solved earlier in section 4.2. The solution would not necessarily be the same, however, since the boundary conditions would be different. Nonetheless, scaling has shown that the principle forcing comes from vertical ocean current shear. In the case of surface currents with shear (section 4.2) we found that the horizontal-shear forcing is generally of order $\lambda/\mu = \alpha \ll 1$ compared to the vertical-shear forcing (λ is the cross-flow horizontal wave number and $1/\mu$ was the velocity depth decay scale that was used in that problem). This is also found here in the scaling arguments. Hence, where $F_z \ll F_y$ (such as at or within a couple of degrees of the magnetic equator) we will expect that the horizontal-shear forcing will be dominant.

5.1 Importance of Bathymetry and Baroclinicity

Let us assume that $H = H(x, y)$; $\mathbf{u} = \mathbf{u}(x, y, z)$, $w = 0$; and $\sigma = \sigma(x, y)$ within the water and $\sigma = 0$ everywhere else. Also, let $b_z \ll F_z$ so that we can take $B_z \approx F_z = F_z(x, y)$. We note that if the ocean currents remain strong close to the seafloor, and where there is variable bathymetry, the approximation $w = 0$ above may not remain valid. Here, however, we will primarily be interested in the effect of bathymetry on the recirculation of electrical charge separated by ocean surface currents. Hence we are concentrating on the importance of bathymetry in controlling the electrical flow rather than the fluid flow.

We combine 66 and 67 into a vector equation and integrate with respect to depth to yield

$$\mathbf{B}_H = -\sigma\mu_o F_z \int_{-H}^z \mathbf{u} dz - \mathbf{M}_1(x, y) \frac{z}{H} + \mathbf{M}_2(x, y) \quad (69)$$

where \mathbf{M}_1 and \mathbf{M}_2 are functions to be determined.

At the sea surface and ocean floor there can be no electrical flow across the boundaries. This can be stated as

$$(\nabla \times \mathbf{B}) \cdot \hat{z} = \nabla \times \mathbf{B}_H = 0 \quad \text{for } z = 0, -H. \quad (70)$$

A solution to 69 subject to 70 is

$$\mathbf{B}_H = F_z \sigma \mu_o \mathbf{T} \left[-\frac{1}{T} \int_{-H}^z u dz + \left(1 + \frac{z}{H}\right) \right] - \frac{z}{H} \mathbf{N}_1(\mathbf{x}, \mathbf{y}) + \left(1 + \frac{z}{H}\right) \mathbf{N}_2(\mathbf{x}, \mathbf{y}) \quad (71)$$

where u and T are the magnitudes of \mathbf{u} and \mathbf{T} , respectively, and \mathbf{N}_1 and \mathbf{N}_2 are irrotational vectors to be chosen.

We will discuss for a moment the significance of the vectors \mathbf{N}_1 and \mathbf{N}_2 . First notice that the term in square brackets in 71 vanishes at the sea surface or sea floor. Then, the vectors \mathbf{N}_1 and \mathbf{N}_2 are the values of \mathbf{B}_H at the ocean floor and sea surface, respectively. Also, since \mathbf{B}_H must be continuous across the boundary, \mathbf{N}_1 and \mathbf{N}_2 serve as a matching condition for the large-scale problem of magnetic flux continuity. In other words, our scaling analysis showed that the magnetic fields within the ocean are primarily dependent on the local ocean current shear (as well as the local value of the other field parameters). Or, more accurately, the charge separation is a local effect occurring in the areas of local current shear. The paths of return electrical flow, however, are not necessarily local. This is shown by the fact that we can only solve the local problem to within some undetermined field that is irrotational in the horizontal plane, representing the horizontal return flow of electric charge. To solve the problem completely, either the global configuration must be solved for or—and easier for the purpose of illustration—some assumptions about the returning electrical flow must be made.

In particular, note that we have written \mathbf{B}_H in the form given in 71 so that setting $\mathbf{N}_1 = \mathbf{N}_2$ is equivalent to assuming that all charge separated in the region of ocean currents returns along paths directly below in the deeper water. If the along-flow variations are small, both of these vectors, aside from being equal, are also zero. (This is what occurs in the solution we found shown in figure 6.) The fact that there often exist substantial along-flow variations (especially in H and F_z) will be used as an argument later to suggest that substantial magnetic flux must leak out of the water. For the moment we return to the local problem.

Contrary to the case of complete charge return, if we set $\mathbf{N}_1 = -\mathbf{N}_2$ this is equivalent to the assumption that *no* charge returns below and this profile would be similar to the infinite-plane case we studied (solution plotted in figure 4).

We can also show, to the same scaling approximations, upon integrating equation 19 over the depth that the total electrical current (per unit of ocean length) flowing in the ocean layer H is simply

$$\int_{-H}^0 \mathbf{J} dz = \frac{1}{\mu_o} (\mathbf{N}_2 - \mathbf{N}_1), \quad (72)$$

from which the earlier assertions regarding \mathbf{N}_1 and \mathbf{N}_2 are supported.

Assuming the velocity profile $u = u_o(x, y)e^{\mu z}$, $\mathbf{N}_1 = \mathbf{N}_2 = 0$, and noting

$$\mathbf{T} = \frac{\mathbf{u}_o}{\mu} (1 - e^{-\mu H}), \quad (73)$$

equation 71 can be written in terms of the surface velocity

$$\mathbf{B}_H = F_z \sigma \mu_o \frac{u_o}{\mu} \left[-e^{\mu z} + e^{-\mu H} + (1 - e^{-\mu H})(1 + z/H) \right], \quad (74)$$

or the transport \mathbf{T}

$$\mathbf{B}_H = F_z \sigma \mu_o \mathbf{T} \left[-\frac{(1 - e^{\mu(z+H)})}{(1 - e^{\mu H})} + 1 + z/H \right]. \quad (75)$$

The velocity and magnetic-field profiles are shown in figure 12.

For a given transport T we can ask how the shape of the magnetic-field profile depends on the ratio $D/H = 1/(\mu H)$. This is seen by plotting equation 75 in units of H as shown in figure 13. We see that as the flow becomes more barotropic (depth-independent), magnetic induction is no longer as efficient.

From the magnetic profile given in 75, we can calculate the associated electric current density and electric field. The horizontal electric current density field can be easily calculated from 19. It is

$$\mathbf{J}_H = F_z \sigma \mu_o T \left[\frac{\mu e^{\mu(z+H)}}{(1 - e^{\mu H})} + 1/H \right] (\hat{T} \times \hat{z}), \quad (76)$$

where \hat{T} is the unit vector in the direction of the transport.

Equation 76 together with 75 can then be used in 13 to calculate the electric field. Both the electric field and current density are also given in figure 13.

Vertical Integration:

We can integrate 71 through the depth of the ocean to get

$$\int_{-H}^0 \mathbf{B}_H dz = F_z \sigma \mu_o \left[- \int_{-H}^0 \int_{-H}^z \mathbf{u}(z') dz' dz + \mathbf{T} \frac{H}{2} \right] + (\mathbf{N}^*) H \quad (77)$$

where

$$\mathbf{N}^* = \frac{\mathbf{N}_1 + \mathbf{N}_2}{2}, \quad (78)$$

which is similar to the \mathbf{J}^* currents discussed by Sanford (1971).

Equation 77 shows that the magnetic fields generated by the ocean depend not only on the transport but also on the vertical shear of the flow. When $D \ll H$, the first term in the brackets in 77 will be much smaller than the second and we can write

$$\int_{-H}^0 \mathbf{B}_H dz \approx [F_z \sigma \mu_o \mathbf{T} + \mathbf{N}^*] H/2. \quad (79)$$

But as the flow becomes barotropic there is no return flow of electrical charge under the ocean currents and the magnetic profile within the ocean will be a linear connection between \mathbf{N}_2 at the surface and \mathbf{N}_1 at the ocean floor.

In general, we can define

$$\tilde{H} = -2/T \int_{-H}^0 \int_{-H}^z u(z') dz' dz + H, \quad (80)$$

and interpret \tilde{H} as an effective depth that depends on both baroclinicity and relief.

Then we can write 77 as

$$\vec{\phi}_l = 2F_z \sigma \mu_o \mathbf{T} \tilde{H}. \quad (81)$$

We interpret

$$\vec{\phi}_l = \int_{-H}^0 \mathbf{B}_H dz - \mathbf{N}^* H \quad (82)$$

as the magnetic flux through the ocean depth due to local sources.

For the exponential and step velocity profiles shown in figure 5, \tilde{H} has the form

$$\tilde{H} = 2 \frac{u_o}{T} \left(\frac{1}{\mu^2} (1 - e^{-\mu H}) - \frac{H}{\mu} e^{-\mu H} \right) + H = \frac{H}{e^{\mu H} - 1} - \frac{1}{\mu} + H, \quad (83)$$

and

$$\tilde{H} = H - D \quad (84)$$

respectively.

For purely baroclinic flow ($\mathbf{T} = 0$) equation 83 should be used and μ is complex.

Note from 83 and 84 that as the flow becomes depth independent (barotropic) (by letting $\mu H \rightarrow 0$ or $D \rightarrow H$), we have $\tilde{H} \rightarrow 0$ indicating that the magnetic field is approximately linear with depth (given by \mathbf{N}_1 and \mathbf{N}_2) and there is no charge recirculation at lower depths. On the other hand, when $D/H \rightarrow 0$, then $\tilde{H} \rightarrow H$.

Using 84 in 81 we obtain a simple expression for the magnetic flux generated by ocean surface currents:

$$\vec{\phi}_l = F_z \sigma \mu_o \mathbf{T} \tilde{H} \approx F_z \sigma \mu_o \mathbf{T} H. \quad (85)$$

Contrary to the approximation 85 for currents confined to the ocean surface, we see that for barotropic flow there is no net magnetic flux in the horizontal

direction since $\tilde{H} = 0$ —regardless of the transport. Hence consideration of the ocean current vertical profile is mandatory and this dependence can easily be included by using \tilde{H} instead of H .

5.2 Importance of Variations in Conductivity and the Vertical Component of the Earth's Magnetic Field F_z

We have seen that the charge separation depends essentially on the product $F_z\sigma u$. However, to consider the electrical currents and magnetic field generated we are interested in variations in $F_z\sigma u$.

There are probably cases in the global oceans where any one of the components in the product $F_z\sigma u$ (and \tilde{H}) is dominant. At the interface between ocean and air or ocean and land, certainly this product will be dominated by the change in conductivity over the interface. Even within the flow, however, we can expect that variations in the conductivity field (which can be as high as a factor of two) may be as important as variations within the velocity field.

On a global scale, there are probably some systematic effects of conductivity transport. For example, the ocean is known to transport heat (and, hence, conductivity) poleward. This should have the net effect of creating a global electric current with positive charge moving westward. Since the conductivity is higher in the warmer low latitudes, this electric current may be more concentrated there. The continents have a much lower conductivity and would certainly have a large effect on this electric current attempting to move westward. The natural paths for these currents encountering continents would be through areas with the highest conductance (areas with more water than land, in particular). It is interesting to speculate that the conductance of the Central American Isthmus or of the Middle East might have changed when the Panama and Suez canals were constructed (and expanded). If an electric current due to the systematic transport of conductivity regularly circles the globe, contributing to the earth's magnetic

field, then the magnetic field might be affected by these constructions. Particularly, the construction of the Panama Canal in 1912 and the temporary closure of the Suez Canal between the late 1960's and mid 1970's might be related to the unexplained magnetic 'jerks' that have been reported for similar dates.

The earth's main vertical field F_z , while it can probably be taken as uniform at the poles, is varying considerably at low latitudes. Hence, for equatorial currents away from boundaries, variations in the product $v\partial_y F_z \approx vF_o/R_E$ (where R_E is the earth's radius) may dominate induction. This may lead to a great simplification in the analysis of induction by equatorially- trapped waves.

5.3 Leakage of Magnetic Field out of the Ocean

Since the \mathbf{B} field is nondivergent, we can write

$$\delta B_z = -\nabla \cdot \int_{-H}^0 \mathbf{B}_H dz \approx -\nabla \cdot \left\{ \left(\frac{1}{2} F_z \sigma \mu_o \mathbf{T}\tilde{H} + \mathbf{N}^* H \right) \right\} \quad (86)$$

where δB_z is the change in B_z across the ocean depth ($B_z(z=0) - B_z(z=-H)$).

We want to argue that the ocean-induced magnetic fields are not confined to the ocean. This is important since it may be possible that magnetic records taken at land observatories contain information about present and past ocean circulation.

First suppose that the magnetic fields *are* confined to the ocean. For this we must have δB_z in 86 equal to zero. Now although \mathbf{N}^* must be irrotational, the vector $F_z \sigma \mathbf{T}\tilde{H}/H$ is, in general, not. Hence, we see that we can not reasonably assume that δB_z in 86 will vanish. Stated another way, when the conductivity transport crosses isobaths or lines of equal F_z , or even with changes in the baroclinic structure of the flow, we can usually expect leakage of the magnetic flux out of the ocean.

An example:

When the along-stream variations are not too abrupt, \mathbf{N}_1 is probably much smaller than $F_z \sigma \mu_o H \mathbf{T}$. This can be seen from the fact that \mathbf{N}_1 lies in a horizontal plane and must be curl-free. Hence, if the variations are zero alongshore then $\mathbf{N}_1 = 0$. This was found in the analytic solutions of section 4. The smoother features of magnetic flux leakage at the surface may then be roughly estimated by the expression

$$\delta B_z \approx -\nabla \cdot \left\{ \frac{1}{2} F_z \sigma \mu_o \mathbf{T} H \right\}. \quad (87)$$

This can be used as a boundary condition while seeking a solution to

$$\nabla^2 \mathbf{B} = 0, \quad (88)$$

which is applicable in the insulating regions outside of the ocean.

Let's consider an illustration of magnetic flux leakage due to along-flow variations.

Let's assume, for example, that the conductivity structure of the mixed layer has a sinusoidal variation along the flow. (Or, we could for example assume a sinusoidal variation in D and hence \tilde{H} .) We also will neglect cross-flow variations for the moment. We write

$$\sigma = \sigma_o(1 + a e^{ikx}), \quad \mathbf{T} = T \hat{x}. \quad (89)$$

We will also assume $b_z(z=0) \approx \frac{1}{2} \delta B_z$, $b_z(z=-H) \approx \frac{-1}{2} \delta B_z$, and $F_x = F_y = 0$. Then, solving 88 using 87 and 89 while requiring that the solution remain bounded at infinity, we find that the solutions are the real part of the following expressions. In the air

$$\mathbf{B} = \frac{1}{2} \delta B_z e^{-kz} [-i \hat{x} + \hat{z}] + F_z \hat{z}, \quad (90)$$

and below the ocean floor

$$\mathbf{B} = \frac{-1}{2} \delta B_z e^{k(z+H)} [i \hat{x} + \hat{z}] + F_z \hat{z}, \quad (91)$$

where $\delta B_z = -\frac{1}{F_z \mu_o H T i k a \sigma_o e^{ikz}}$. (An example of this solution is shown in figure 14a . A similar calculation for induction by the double gyre shown in figure 10 is also calculated and is shown in figure 14b.)

From this calculation—though very rough—we can estimate the magnitude of the magnetic field in the air. First note that the magnitude within the water is of order $\sigma \mu_o F_z |\mathbf{T}|$ which, using typical values, tells us that in the water the ocean-induced fields will have about the same magnitude (in nT) as the transport (in m^2/s)—this is useful to remember. Outside of the water the fields are reduced by a factor of about H/\mathcal{L}_a . If we consider the Gulf Stream (with transport per unit width of $T \approx 10^3 m^2/s$, $H \approx 5 \times 10^3 m$) and take the conductivity variations to vary as $\mathcal{L}_a \approx \frac{1}{ak} \approx 1 \times 10^4 m$, we would find the magnetic fields to be of order 1000 nT in the water and 100 nT outside of the water.

This last number represents a high-side estimate since few current systems are as strong and deep as the Gulf Stream. On the other hand, along-stream variations (especially in H) can be much more abrupt than we have supposed here, so ocean-induced magnetic fields penetrating into the air of order 100 nT may be quite common.

5.4 When Vertical Motions are Important

We assumed above that the vertical velocities were very small. If we consider motions such as tides, storm surges, time variations in coastal setup, coastal upwelling, or perhaps even areas in the thermohaline circulation where strong sinking events occur, then instead of 68 we might have the following balance.

$$\partial_z \partial_z B_z = -R_{m,c} \frac{\alpha \alpha_w}{\alpha_m} B_z \partial_z w. \quad (92)$$

(This can be derived using as an example for tides using a value $w \approx 1$ meter per day, and also assuming for this case that we are dealing with a smaller horizontal scale over which the horizontal conductivity gradients are small.)

Assuming $B_z \approx F_z$ and that the fluid is incompressible, 92 can be written as

$$\partial_z \nabla_H \cdot \mathbf{B} = -\frac{\alpha_w}{\alpha_m} R_{m,c} F_z \nabla_H \cdot \mathbf{u}. \quad (93)$$

Equation 93 shows that for cases of large vertical velocities and small horizontal variations in conductivity, we might observe a correlation between the vertical variations of the horizontal magnetic divergence and the horizontal divergence of the flow.

6 Discussion

Ocean currents induce magnetic fields that are probably contained in the geomagnetic record. The purpose of this report series is to extend the theory of ocean-induced electromagnetic fields with the aim of examining the potential for using geomagnetic data in ocean and climate studies.

In later *C²GCR* reports we will eventually be lead to more realistic results using numerical models. First, however, we feel it is important to gain physical insight into the processes involved. We pursue this by working with analytical results and investigating special cases.

In this report we combine Maxwell's equations (together with some parameterizations) into an induction equation allowing for variable conductivity. We use the theory established in magnetohydrodynamics to scale the electromagnetic variables and the theory established in oceanography to scale the oceanic variables.

We find that the ocean induces fields that probably average of order 1 to 100 nanoteslas in the water but may, particularly in regions of strong deep-reaching currents, reach magnitudes much greater. This is comparable to the results found in Lilley (1993), for example.

Depth-independent 'barotropic' ocean currents characteristically circulate electrical charge in the horizontal plane leading to induction of a vertical magnetic

component. When there is vertical shear in the ocean current, electric charge can recirculate in a plane containing the vertical axis. This can lead to induction of magnetic components in the horizontal plane.

Magnetic fields that are induced in one plane can, however, acquire components normal to this plane as they relax away from their source areas. Hence, when there is strong vertical ocean current shear the portion of the horizontally-induced fields that ‘leak’ out of the ocean may be greater in magnitude to that induced directly by the horizontal electric currents.

In some cases the processes of barotropic and baroclinic induction overlap. In other examples we can construct scenarios with purely baroclinic flow that have zero transport (hence, no barotropic current) which, however, create strong baroclinic induced fields. In general we conclude that a realistic model of the ocean induction must resolve the three-dimensional structure of the currents.

The three dimensional resolution of the the conductivity field is also necessary. While in this report we have considered solutions for only slow and regularly varying changes in conductivity, it is probable that abrupt changes in bathymetry can lead to magnetic fields much larger in magnitude than the ones we have considered.

7 Appendix

We have the equation

$$\frac{d}{dz} \left\{ e^{-\gamma z} \frac{d}{dz} Z \right\} - \lambda^2 e^{-\gamma z} Z = \frac{-i\lambda F_y - \mu F_z}{K_o} u_o e^{\mu z} \quad (94)$$

which we write symbolically as

$$\mathcal{L}(z) = \mathcal{F}(z). \quad (95)$$

We require that the Green’s functions $G(z | \xi)$ satisfy the equation

$$\mathcal{L} \{G(z | \xi)\} = \delta(z - \xi) \quad (96)$$

in the domain $-\infty < z \leq 0$. Here, $\delta(z - \xi)$ is the Dirac delta function. Equation 96 implies that G must satisfy the corresponding homogeneous equation

$$\mathcal{L}\{G(z | \xi)\} = 0 \quad (97)$$

everywhere in the domain except at $z = \xi$. Also, G must satisfy the boundary condition (equations 46, and 47) at $z = 0$ and $z \rightarrow -\infty$.

By definition, the integral of $\delta(z - \xi)$ across the spike at $z = \xi$ is equal to one. Hence, we can integrate 96 as follows

$$\int_{\xi-0}^{\xi+0} \mathcal{L}(G)dz = \int_{\xi-0}^{\xi+0} \delta(z - \xi)dz = 1. \quad (98)$$

The function G must be continuous at $z = \xi$. The derivative $d_z G$, however, is not. When we expand \mathcal{L} in 98, and carry out the integration, the only component of $\mathcal{L}(G)$ that does not vanish when integrated over the spike is the term involving $d_z(e^{-\gamma z} d_z G)$. Then,

$$\int_{\xi-0}^{\xi+0} \mathcal{L}(G)dz = \int_{\xi-0}^{\xi+0} d_z(e^{-\gamma z} d_z G) = 1. \quad (99)$$

If we let $\delta G'$ represent the change of $d_z G$ across the spike, then we can write the condition in 99 as

$$\delta G' = e^{\gamma \xi}. \quad (100)$$

Since G may have a different functional form in the regions above and below the level $z = \xi$, we write G_b for region $-\infty < z \leq \xi$ and G_a for $\xi \leq z \leq 0$. Then since G must also satisfy the boundary conditions $G_b(z = -\infty) = 0$ and $G_a(z = 0) = 0$, this suggests that we construct G using the solutions y_a, y_b of the homogeneous equation

$$\mathcal{L}(y) = 0 \quad (101)$$

that satisfy the boundary conditions in their respective regions, that is $y_a(z = 0) = 0$ and $y_b(z = -\infty) = 0$. Homogeneous solutions are

$$y_a = e^{\frac{\gamma z}{2}} \sinh \frac{\beta}{2} z, \quad (102)$$

$$y_b = e^{\frac{\gamma+\beta}{2}z}. \quad (103)$$

where $\beta = (\gamma^2 + 4\lambda^2)^{\frac{1}{2}}$. This would give

$$G_a = y_a(z)f_1(\xi) \quad (104)$$

and

$$G_b = y_b(z)f_2(\xi) \quad (105)$$

where f_1, f_2 are functions to be determined. Since we require continuity at $z = \xi$, we see

$$f_1(\xi) = Cy_b(\xi), \quad (106)$$

$$f_2(\xi) = Cy_a(\xi) \quad (107)$$

where C is a constant. Then we have

$$G_a = \frac{1}{\beta} e^{\frac{\gamma+\beta}{2}z} e^{\frac{\gamma}{2}\xi} \sinh \frac{\beta}{2}\xi \quad -\infty < z \leq \xi, \quad (108)$$

$$G_b = \frac{1}{\beta} e^{\frac{\gamma}{2}z} \sinh \frac{\beta}{2}ze^{\frac{\gamma+\beta}{2}\xi} \quad \xi \leq z \leq 0, \quad (109)$$

where we have used 106,107,102 and 103 in 104 and 105, and we have chosen C to satisfy the condition 100.

8 Acknowledgements

It is a pleasure to thank David Holland who has been very much involved in this research and has offered many helpful comments. He has also produced figure 3. We also thank Paul Lorrain and Robert Langel who have given us several authoritative ‘tutorials’. This work was supported by the Canadian Natural Sciences and Engineering Research Council.

9 References

Apel, J.R. (1987) *Principles of Ocean Physics*, Academic Press, San Diego. 634 pp.

Beal, H.T. and J.T. Weaver (1970) Calculations of Magnetic Variations Induced by Internal Ocean Waves, *Journal of Geophysical Research*, 75, (33), 6846- 6852.

Bloxham, J. and A. Jackson (1992) Time-Dependent Mapping of the Magnetic Field at the Core-Mantle Boundary, *Journal of Geophysical Research*, 97, (B13), 19537-19563.

Bucha, Václav (1980) Mechanism of the Relations between the Changes of the Geomagnetic Field, Solar Corpuscular Radiation, Atmospheric Circulation and Climate, *Journal of Geomagnetism and Geoelectricity*, 32, 217-264.

Bucha, Václav (1988) Influence of Solar Activity on Atmospheric Circulation Types. *Annales Geophysicae*, 6, (05), 513-524.

Bucha, Václav (1991) Solar and Geomagnetic Variability and Changes of Weather and Climate, *Journal of Atmospheric and Terrestrial Physics*, 53, (11/12), 1161-1172.

Bucha, Václav (1993) Temperature Changes in Relation to Geomagnetic Activity. In *Application of Direct and Indirect Data for the Reconstruction of Climate During the Last Two Millenia*, papers presented at the workshop

of PAGES-Stream I, Geological Institute of Academy of Sciences of Czech Republic, Prague, pp 30-39.

Chave, A.D. and D.S. Luther (1990) Low-Frequency, Motionally-Induced Electromagnetic Fields in the Ocean. *Journal of Geophysical Research*, 95, (C5), 7185-7200.

Filloux, J.H. (1987) Instrumentation and Experimental Methods for Oceanic Studies. In *Geomagnetism II*, editor, J.A. Jacobs, Academic Press, San Diego.

Gubbins, D. and P.H. Roberts (1987) Magnetohydrodynamics of the Earth's Core. In *Geomagnetism I*, editor, J.A. Jacobs, Academic Press, San Diego.

Kennett, J.P. and N.D. Watkins (1970) Geomagnetic Polarity Change, Volcanic Maxima and Faunal Extinction in the South Pacific, *Nature*, 227, 930:932.

Larsen, J.C. (1992) Transport and Heat Flux of the Florida Current at 27° N Derived from Cross-Stream Voltages and Profiling Data: Theory and Observations. *Philosophical Transactions of the Royal Society of LondonA*, 338, 169-236.

Larsen, J.C. and T.B. Sanford (1985) Florida Current Volume Transports from Voltage Measurements. *Science*, 227,302-303.

Luther, D.S. (1991) Low-Frequency, Motionally Induced Electromagnetic Fields in the Ocean 2. Electric Field and Eulerian Current Comparison. *Journal of Geophysical Research*, 96, (C7), 12797-12814.

Lilley, F.E.M. (1986) Barotropic Flow of a Warm-Core Ring from Seafloor Electric Measurements, *Journal of Geophysical Research*, 91, (C11), 12979-12984.

Lilley, F.E.M (1993) Magnetic Signals from an Ocean Eddy. *Journal of Geomagnetism and Geoelectricity*, 45, 403-422.

Longuet-Higgins, M.S., M.E. Stern and H. Stommel (1954) The Electrical Field Induced by Ocean Currents and Waves, with Applications to the Method of Towed Electrodes. Papers in Physical Oceanography and Meteorology. MIT and WHOI, Vol 13, No.1, Cambridge and Woods Hole, Massachusetts. 37 pages.

Lorrain, P., D.R. Corson and F. Lorrain (1988) *Electromagnetic Field and Waves*, W.H. Freeman, New York, 3rd edn.

Mysak, L.A. (1986) El Niño, Interannual Variability and Fisheries in the Northeast Pacific Ocean. *Canadian Journal of Fisheries and Aquatic Sciences*, 43, (2), 464-497.

Sanford, T. B. (1971) Motionally Induced Electric Fields in the Sea. *Journal of Geophysical Research*, Vol. 76, No. 15, 3476-3493.

Sanford, T.B. (1982) Temperature Transport and Motional Induction in the Florida Current. *Journal of Marine Research*, 40, supplement, 621-639.

Sanford, T.B. and R.E. Flick (1975) On the Relationship Between Transport and Motional Electric Potentials in Broad, Shallow Currents. *Journal of Marine Research*, 33, 123-139.

Stephenson, David and Kirk Bryan (1992) Large-Scale Electric and Magnetic Fields Generated by the Oceans. *Journal of Geophysical Research*, 97 (C10), 15467-15480.

Weaver, J.T. (1965) Magnetic Variations Associated with Ocean Waves and Swell, *Journal of Geophysical Research*, 70, (8), 1921-1929.

Wollin, Goesta, William B.F. Ryan and David B. Ericson (1977) Paleoclimate, Paleomagnetism and the Eccentricity of the Earth's Orbit. *Geophysical Research Letters*, 4, (7), 267-270.

Wollin, Goesta, William B.F. Ryan and David B. Ericson (1981) Relationship between Annual Variations in the rate of Change of Magnetic Intensity and Those of Surface Air Temperature, *Journal of Geomagnetism and Geoelectricity*, 33, 545-567.

Figure 1: ENSO and magnetic activity

The square of the time rate of change of the total horizontal component of the earth's magnetic field is used here as an indicator of geomagnetic activity. The series is calculated from the monthly record taken at Port Morseby (western equatorial Pacific), (data supplied by the National Geophysical Data Center, Boulder, Colorado). Also shown are the dates of El Niño warming events together with a letter (**w**weak, **m**oderate, **s**trong) to indicate the strength of the events (El Niño data taken from Mysak (1986))

Figure 2: Electrical conductivity as a function of salinity and temperature

The electrical conductivity of water is shown on a 'T-S diagram' expressing the functional dependence of conductivity on salinity and temperature. See Apel (1987) for the equation and coefficients used. Also shown are points (in the right lower side of the figure) indicating the global range of average surface-layer conductivities (see figure 3).

Figure 3: Electrical conductivity of the global ocean

Shown are the average surface-layer conductivities of the global ocean.

Figure 4: Induction by ocean surface current

In (a) we have the magnetic field due to an infinite current sheet (current directed out of paper), and in (c) the field due to an infinite ocean current sheet with exponential depth decay (shown in (b)). These are described in section 4.

Figure 5: Ocean surface velocity with horizontal shear

Shown is the velocity profile used in calculation of section 4.2.

Figure 6: Induction by ocean surface currents including horizontal shear
 Shown are the analytical solutions for the magnetic field induced by the ocean velocities shown in figure 5. (See section 4.2.) The fields in (a), (b), and (c) are calculated using scale-depths ($1/\gamma$) for the conductivity equal to 0, 5000, and 500 (m), respectively. In (d) we have the same as in (b) but we set $F_z = 0$ so that the induction by the earth's horizontal component F_y can be seen. Note that this field is out of phase with the field induced by F_z and is two orders of magnitude less. In (e) we have the same as in (b) but with the scale depth of the currents at $\mu^{-1} = 2000$ m. Note the magnitude of the field is of order 100 nanoteslas. All calculations use $\mu = 1/200$ m, $\lambda = 2\pi/100e3$ m⁻¹, $u_o = 1$ m/s, $F_y = 30,000$ nT, $F_z = -30,000$ nT, and $\sigma = 5$ S/m unless otherwise indicated. These values might be typical in Northern Hemisphere midlatitudes.. Outside of boundary currents, the typical velocities are closer to $u_o \approx .1$ m/s and the induced magnetic fields would be an order of magnitude smaller.

Figure 7: Electrical field E_y and current density J_y
 Shown are contours for the horizontal electrical current density (a) and electric field (b) for the charge separated by the velocity shown in figure 5. The decay scale for conductivity is zero. In (c) and (d) the J_y and E_y fields are shown respectively for a conductivity decay scale of 1 km. We see that returning charge in the latter case is confined to shallower depths.

Figure 8: Ocean surface currents over insulating ocean bottom
 Shown are the magnetic induction (b), the electric current density (c) and the electric field (d) induced by the current illustrated in (a). (See section 4.3).

Figure 9: Baroclinic mode over insulating ocean bottom
 Shown are the magnetic induction (b), the electric current density (c) and the electric field (d) induced by the baroclinic velocity mode illustrated in (a). Note that while a velocity magnitude of $u_o = 1$ m/s has been used, this magnitude only appears in the induction as a multiplier. Hence, induction magnitudes due to smaller baroclinic velocities can easily be inferred. (See section 4.3).

Figure 10: Double ocean gyre
 A large scale double gyre is shown. the maximum velocities are .1 m/s and the homogeneous current layer is assumed to be 100 meters thick.

Figure 11: Induction by large-scale ocean gyres

The vertical magnetic field induced by the large-scale gyres shown in figure 10 is seen to be quite small. See the text for examples of large induced fields. This field was calculated using equation 59 (approximated as a sum) for an altitude of 1000 km. Since the decay scale with height is similar to the horizontal variation scale, the magnitude at the sea surface will not be much greater than at 1000 km.

Figure 12: Solution when all charge recirculates at depth

In (a) an exponential current profile (solid line) is shown. In (b) the magnetic field is calculated using scaling argument as discussed in section 5.1 with $\mathbf{N}_1 = \mathbf{N}_2 = 0$ (this assumption is equivalent to assuming all charge separated in the ocean surface layer returns in the deeper layers below and that there are no background electrical currents due to sources elsewhere).

Figure 13: Dependence of magnetic profile on D/H

Shown is the dependence of the magnetic profile amplitude B_H (per $F_z \sigma \mu_o T$) on the ratio of the mixed layer to the total water depth $D/H \approx (\mu H)^{-1}$. We see that for large $(\mu H)^{-1}$ the induced field becomes small. This is because the ocean flow becomes more barotropic (uniform with depth) and there is no ‘motionless’ layer in which the electrical charges can flow back in—short-circuiting becomes impossible. The only magnetic fields possible are then due to electrical charges flowing through the domain (then \mathbf{N}_1 and \mathbf{N}_2 are not zero).

Figure 14: Leakage of magnetic field out of ocean

Shown in (a) is an example of solution for magnetic field leakage due a wavy variation in conductivity (see section 5.3). Parameters used are $T = 200 \text{ m}^2/\text{s}$, $F_z = 30,000 \text{ nT}$, and $\sigma_o = 5 \text{ S/m}$; $k = 2\pi/(60000) \text{ m}^{-1}$, $a = .5$. A profile of the magnitudes of the induction is shown on the left. In (b) we show a similar calculation for the large-scale ocean gyres illustrated in figure 10.

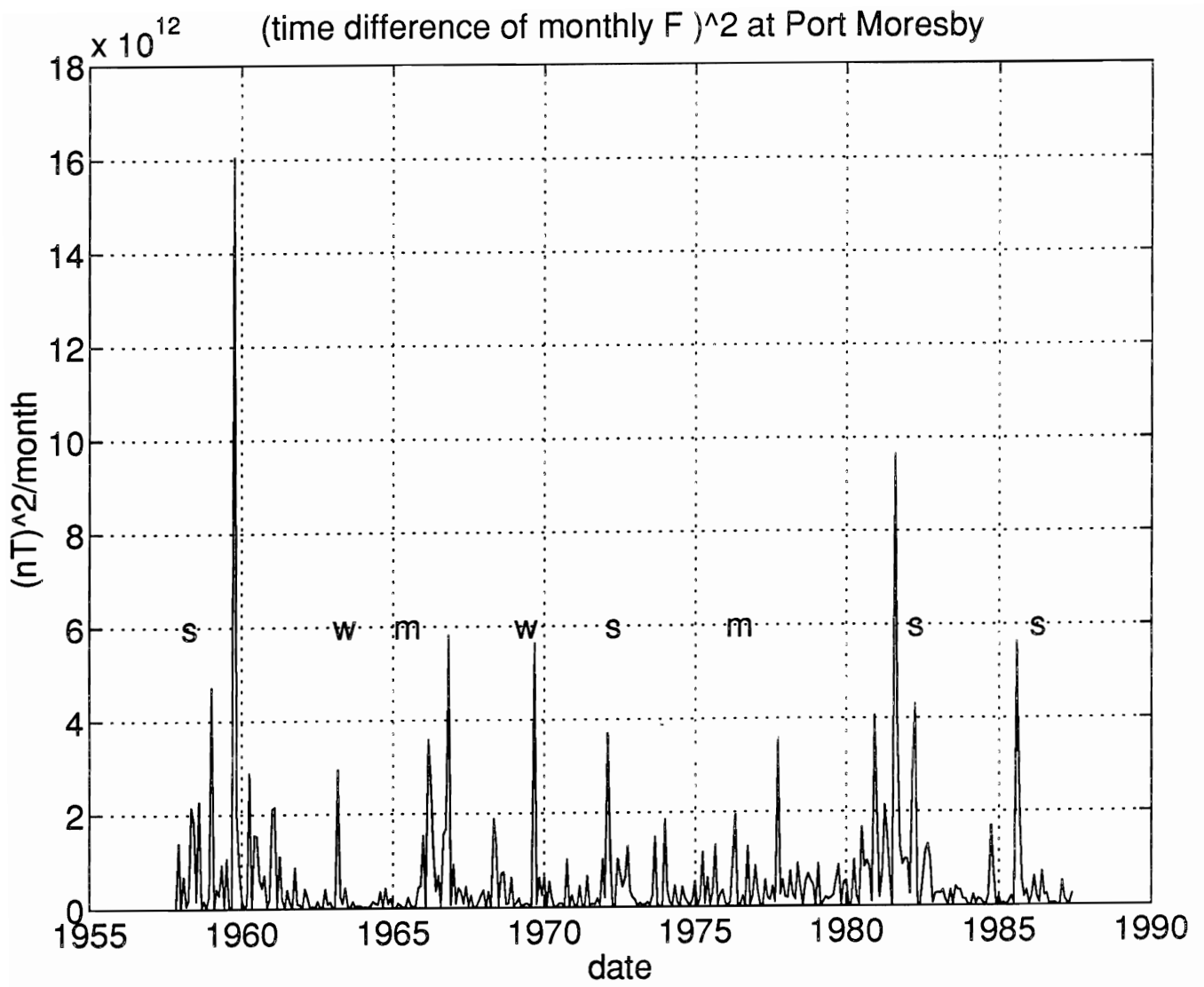


Figure 1

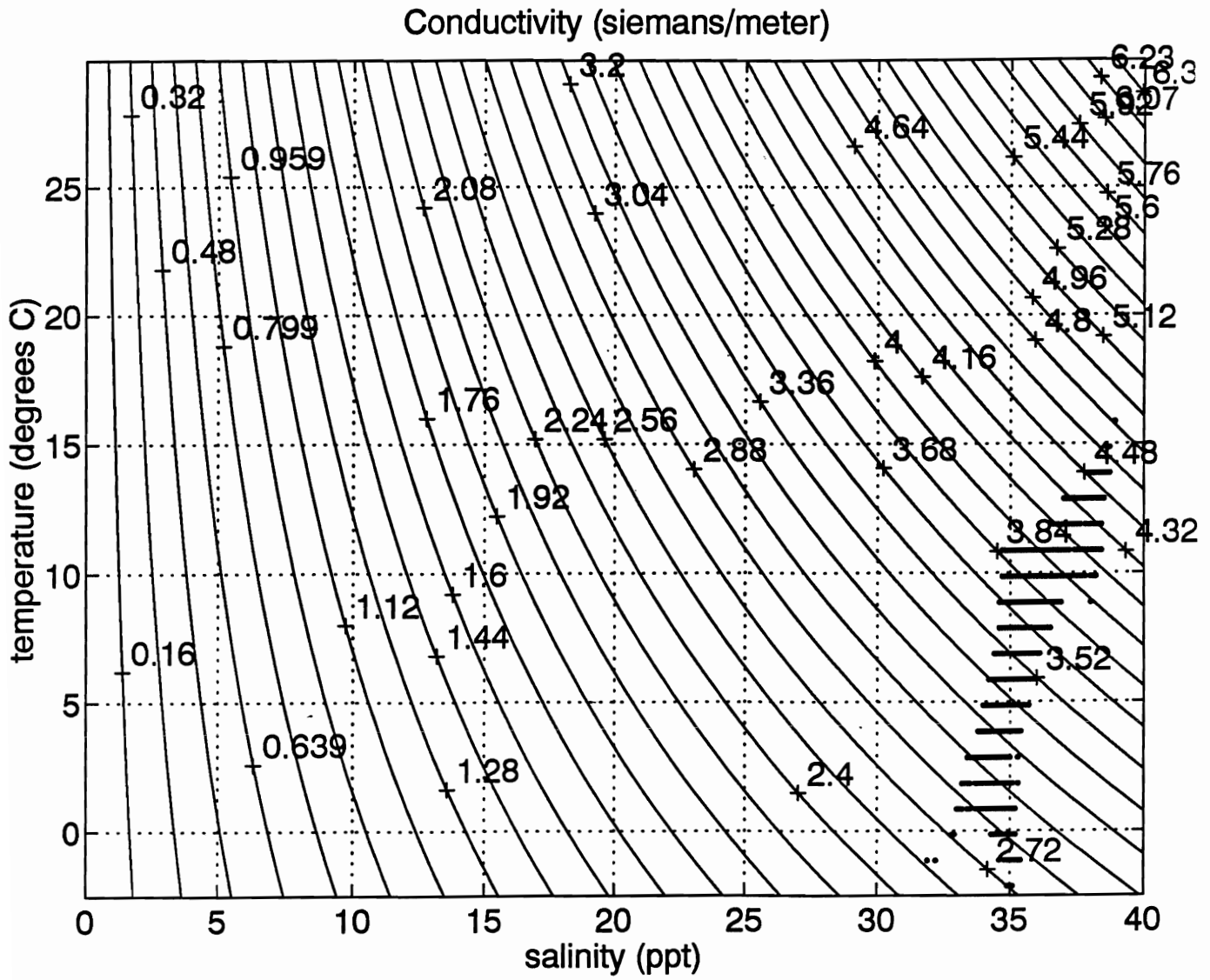


Figure 2

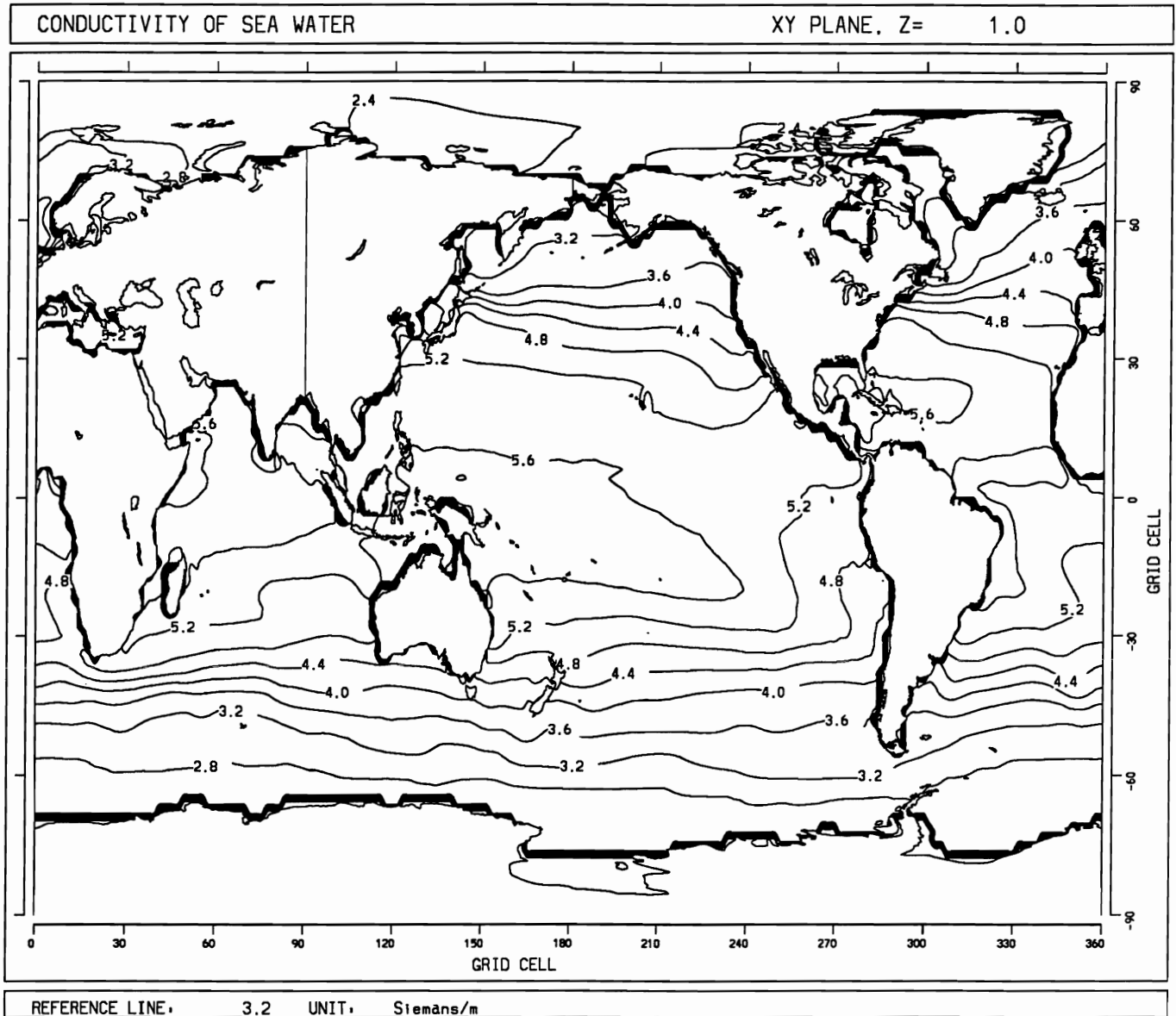


Figure 3

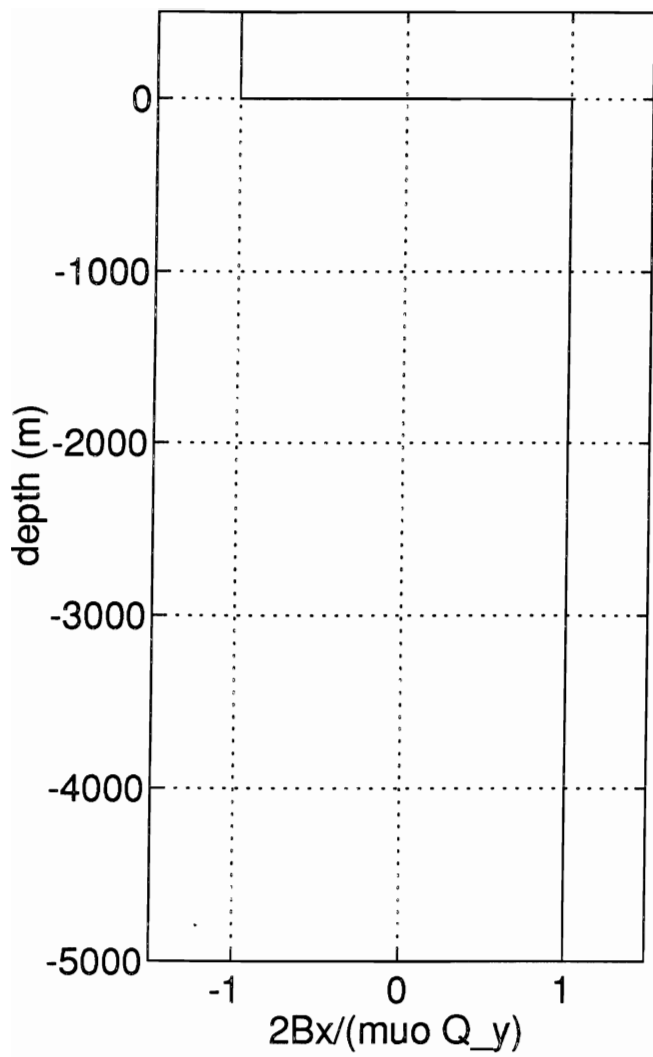


Figure 4 (a)

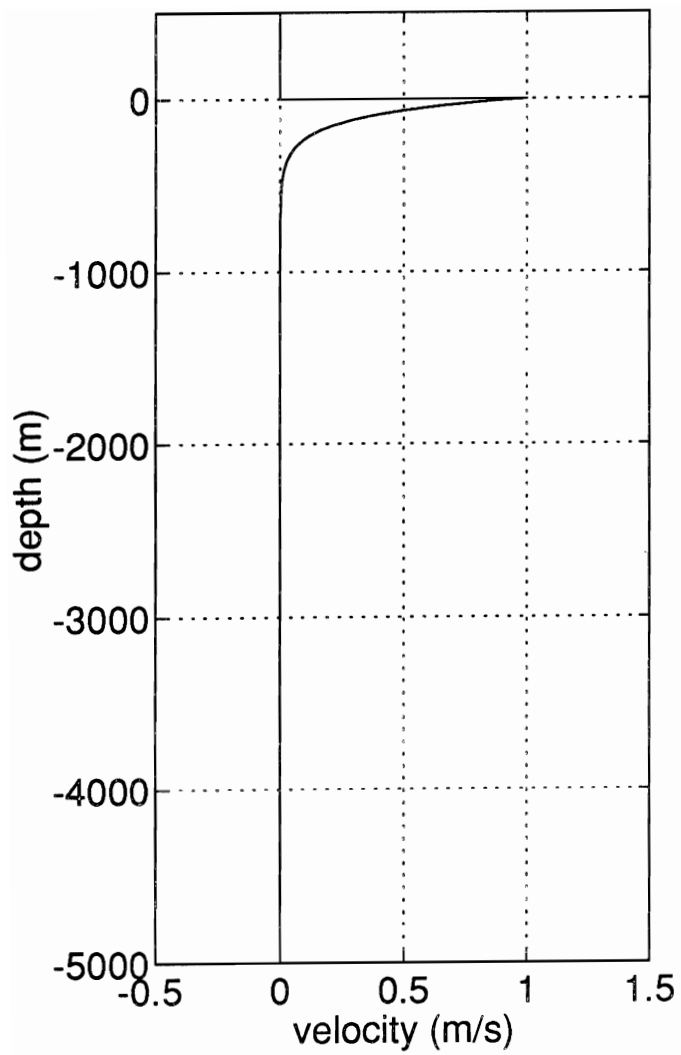


Figure 4 (b)

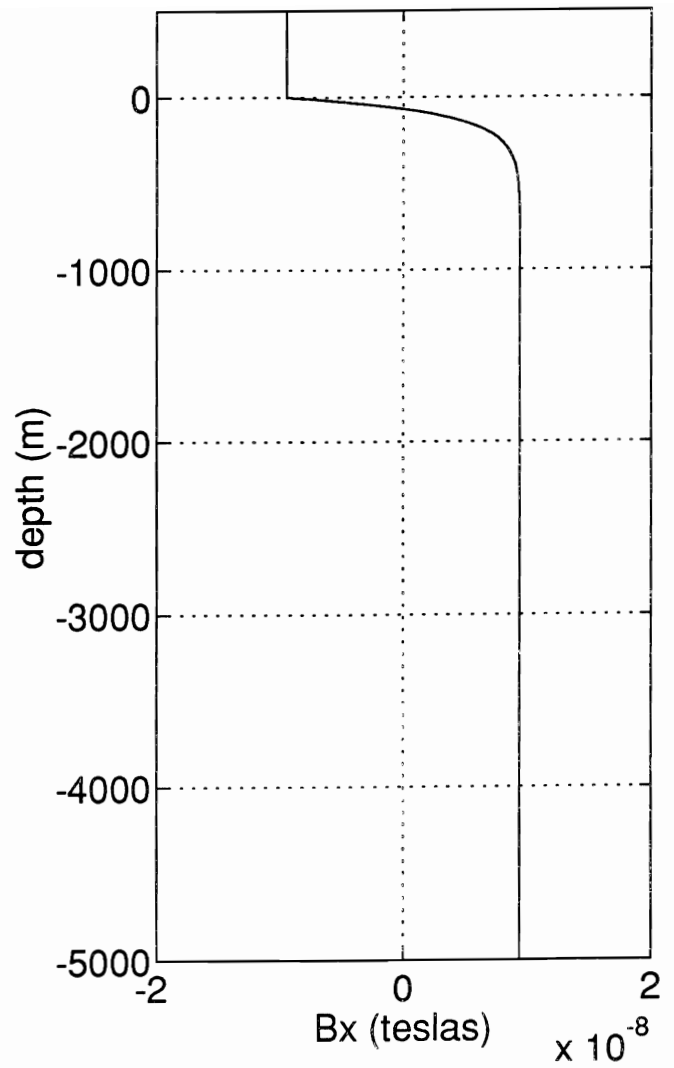


Figure 4 (c)

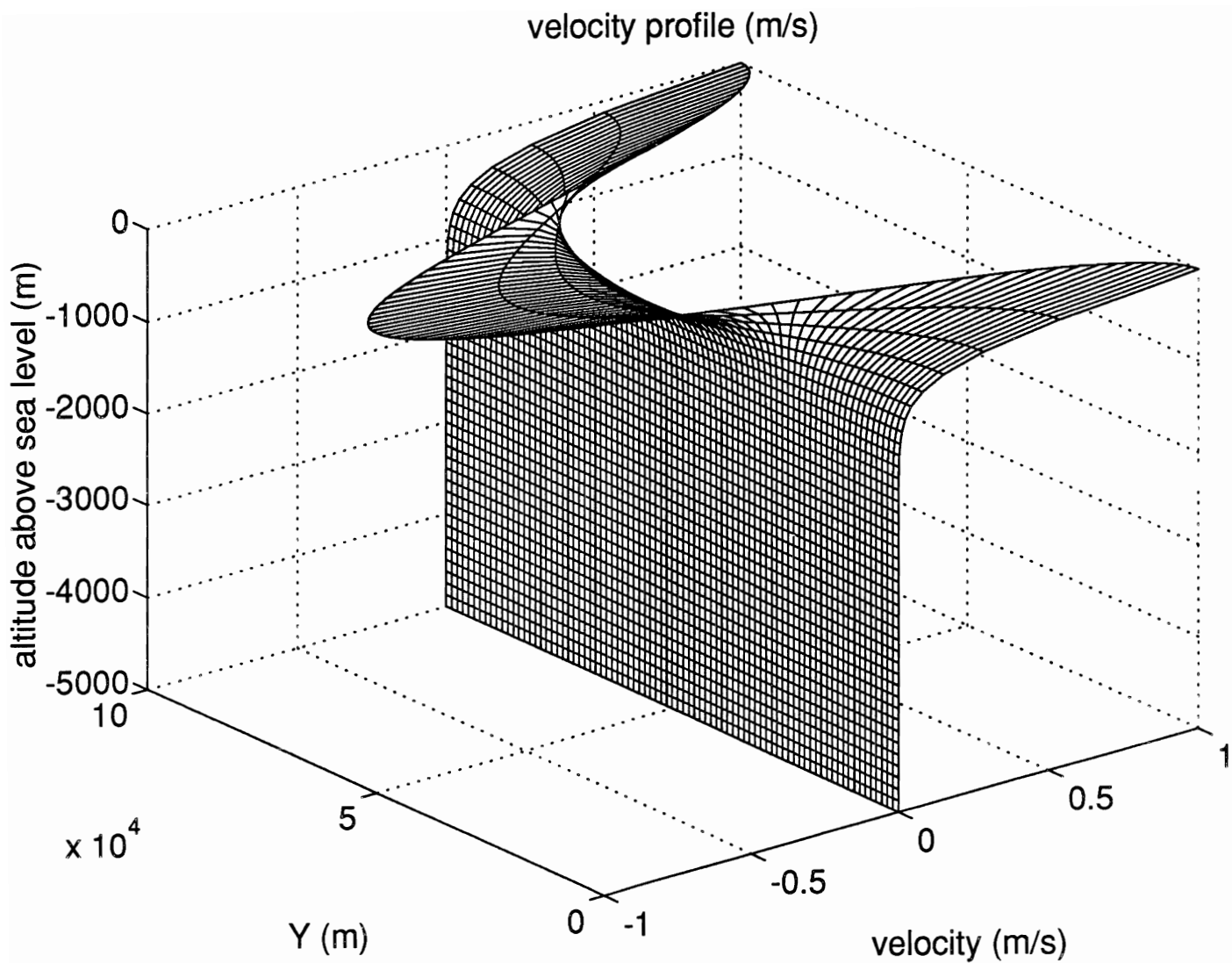


Figure 5

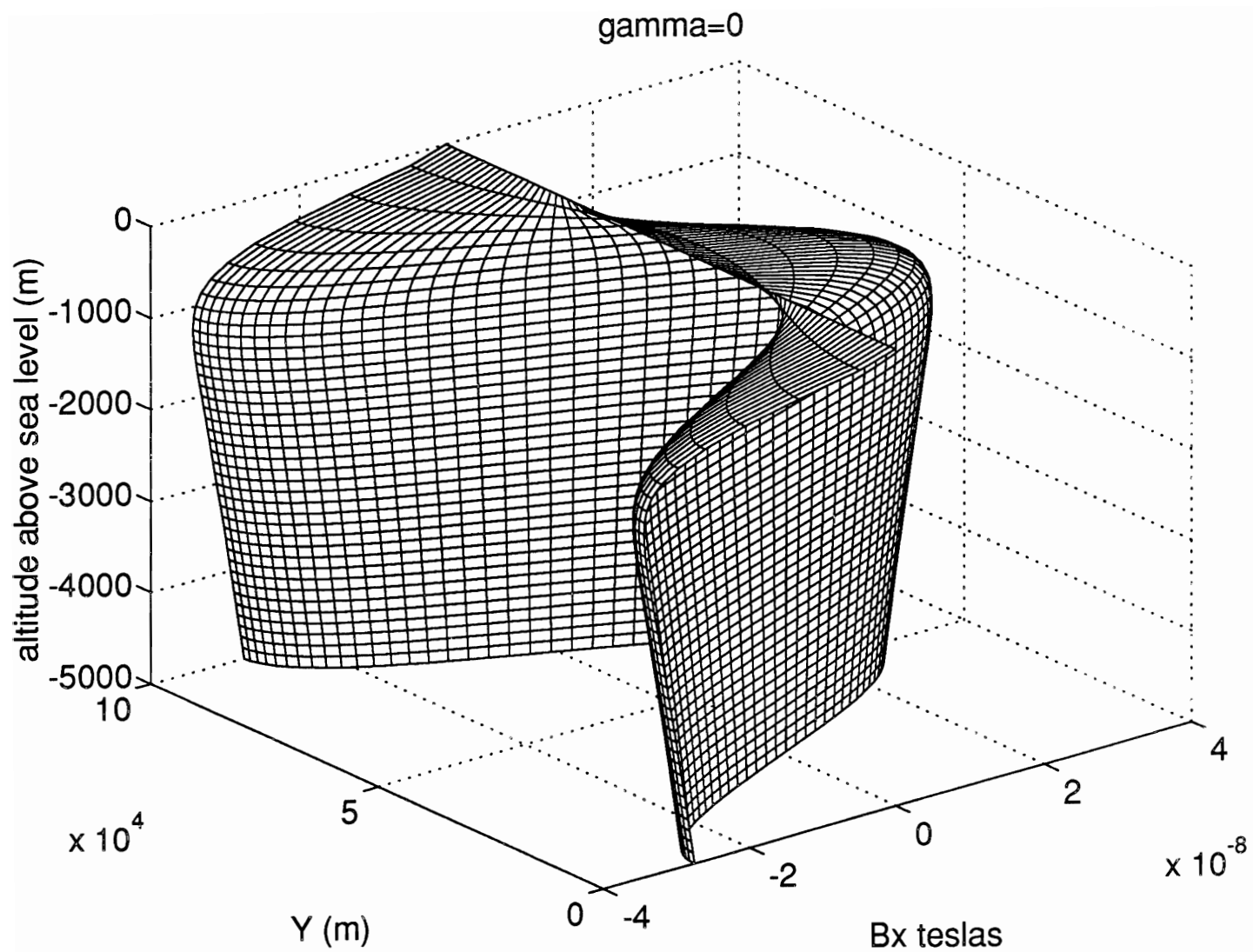


Figure 6 (a)

gamma=1/5000

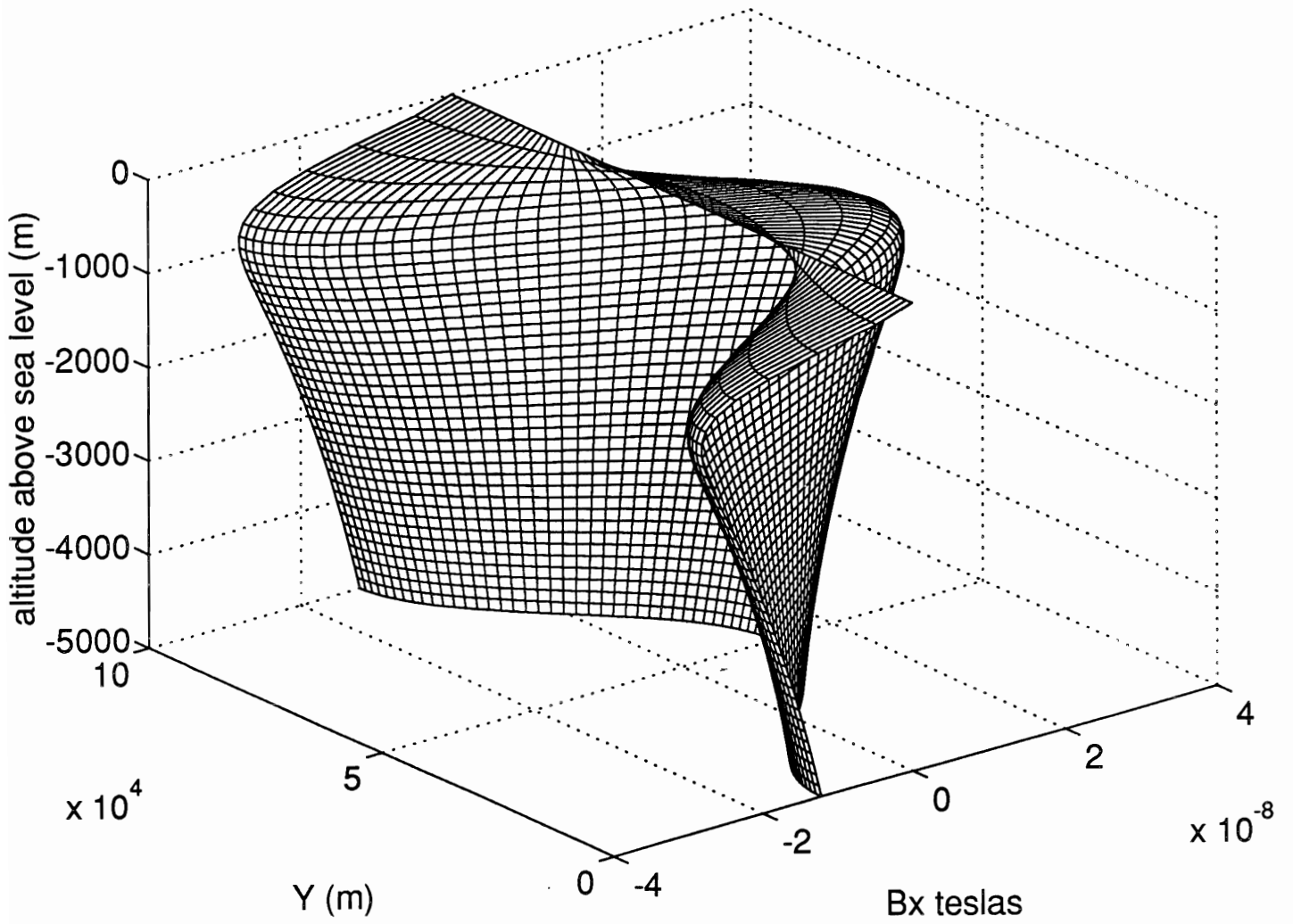


Figure 6 (b)

gamma=1/500

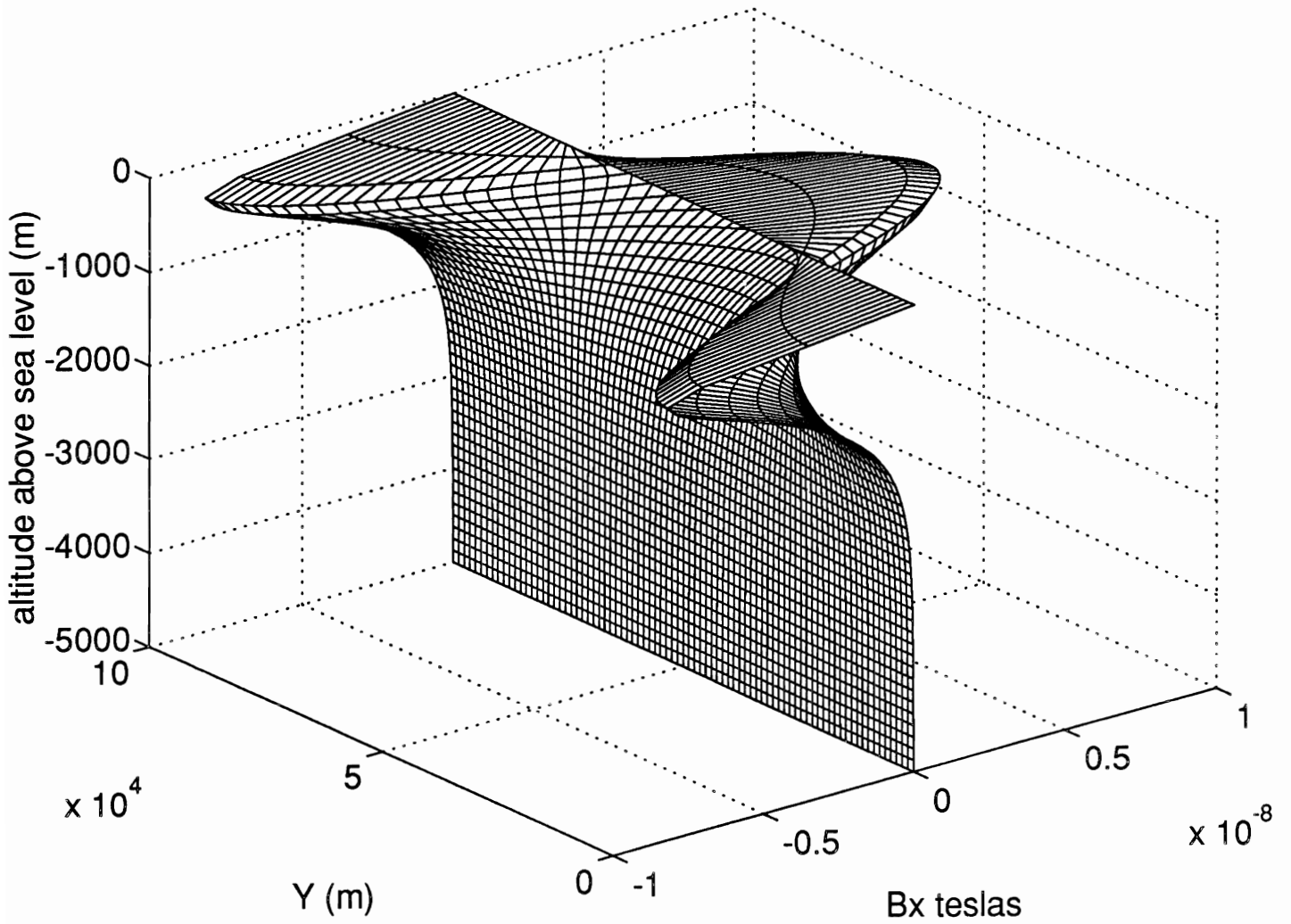


Figure 6 (c)

$\gamma=1/5e3; Fz=0$

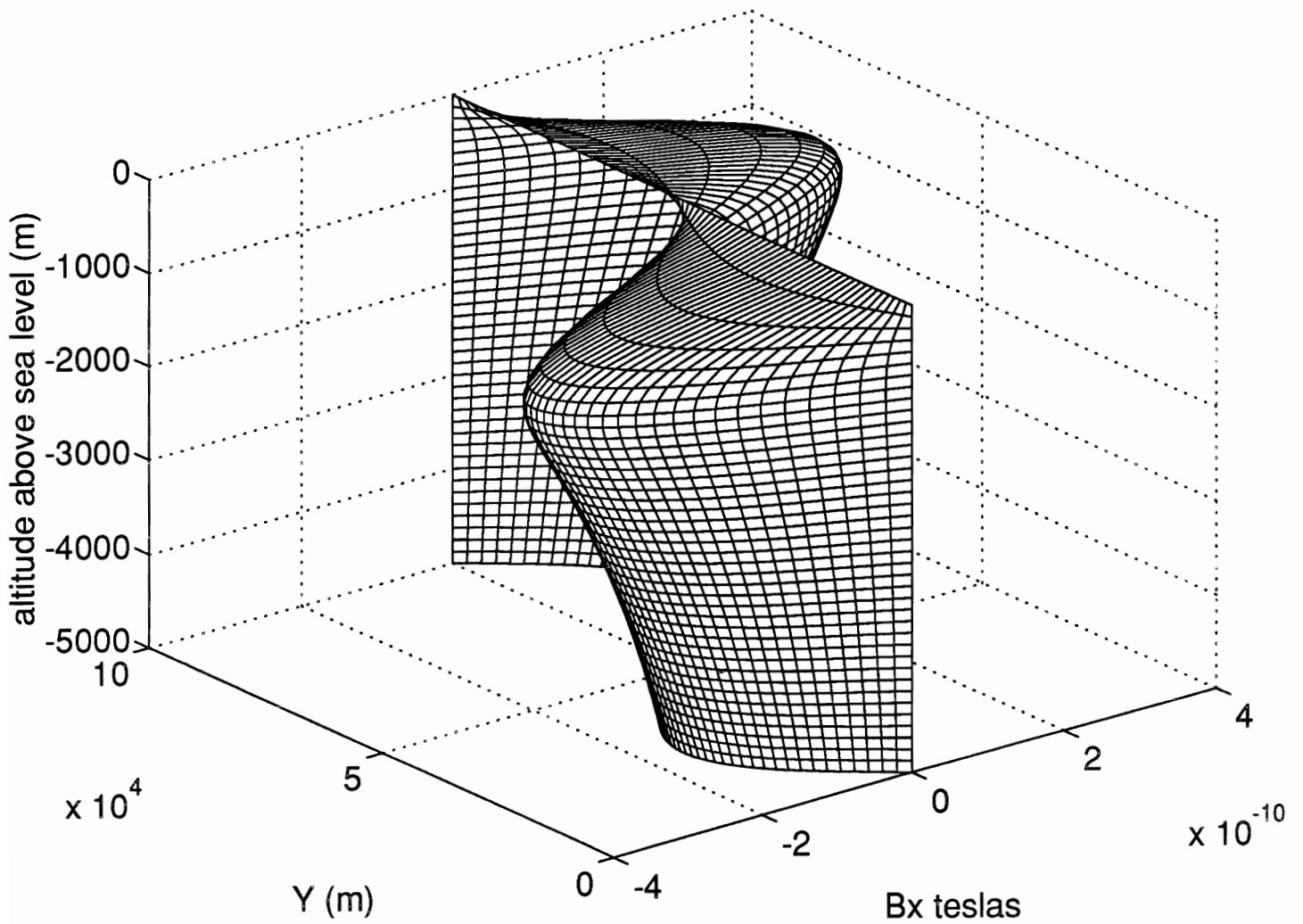


Figure 6 (d)

$\gamma=1/5e3; \mu=1/2000$

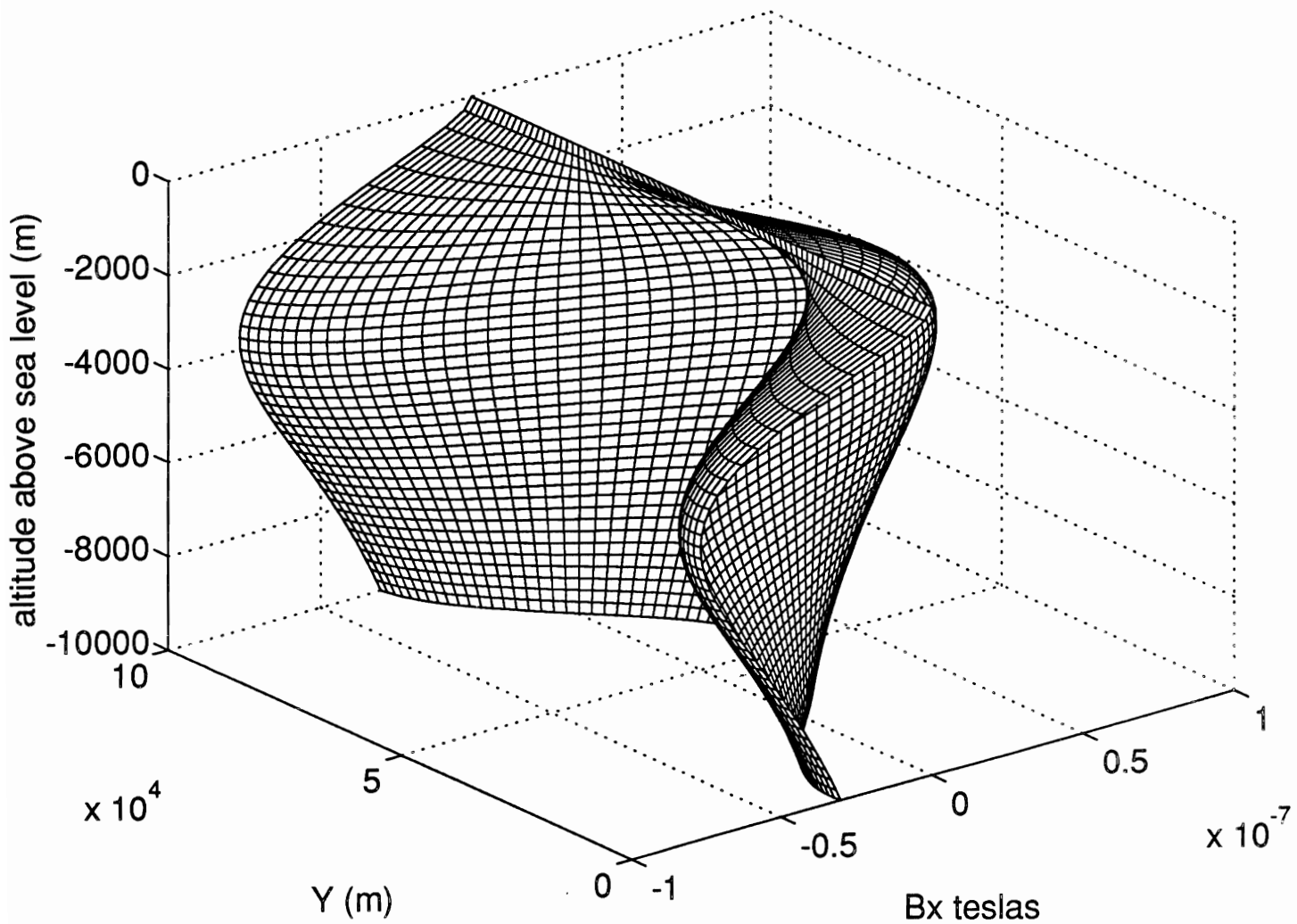


Figure 6 (e)

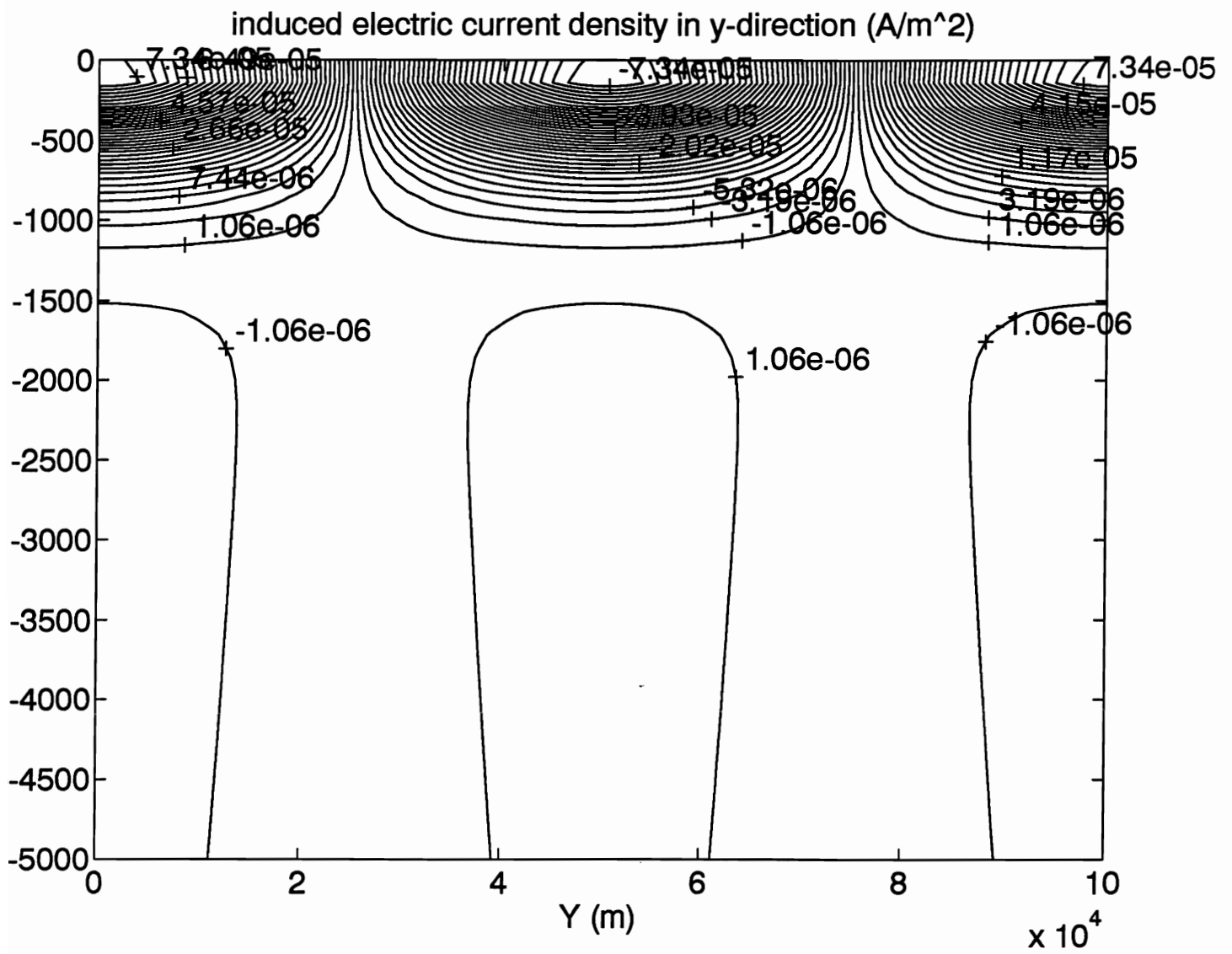


Figure 7 (a)

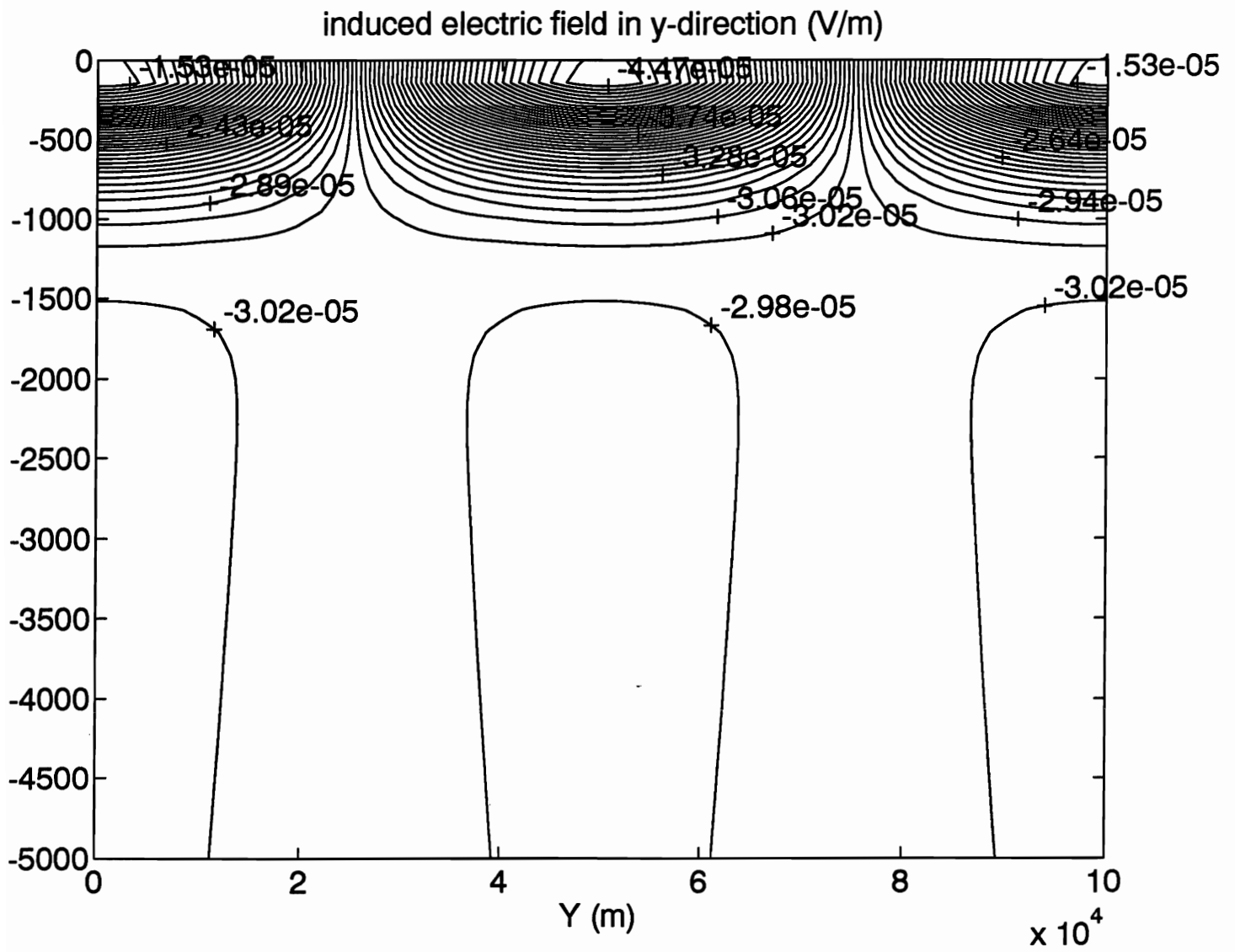


Figure 7 (b)

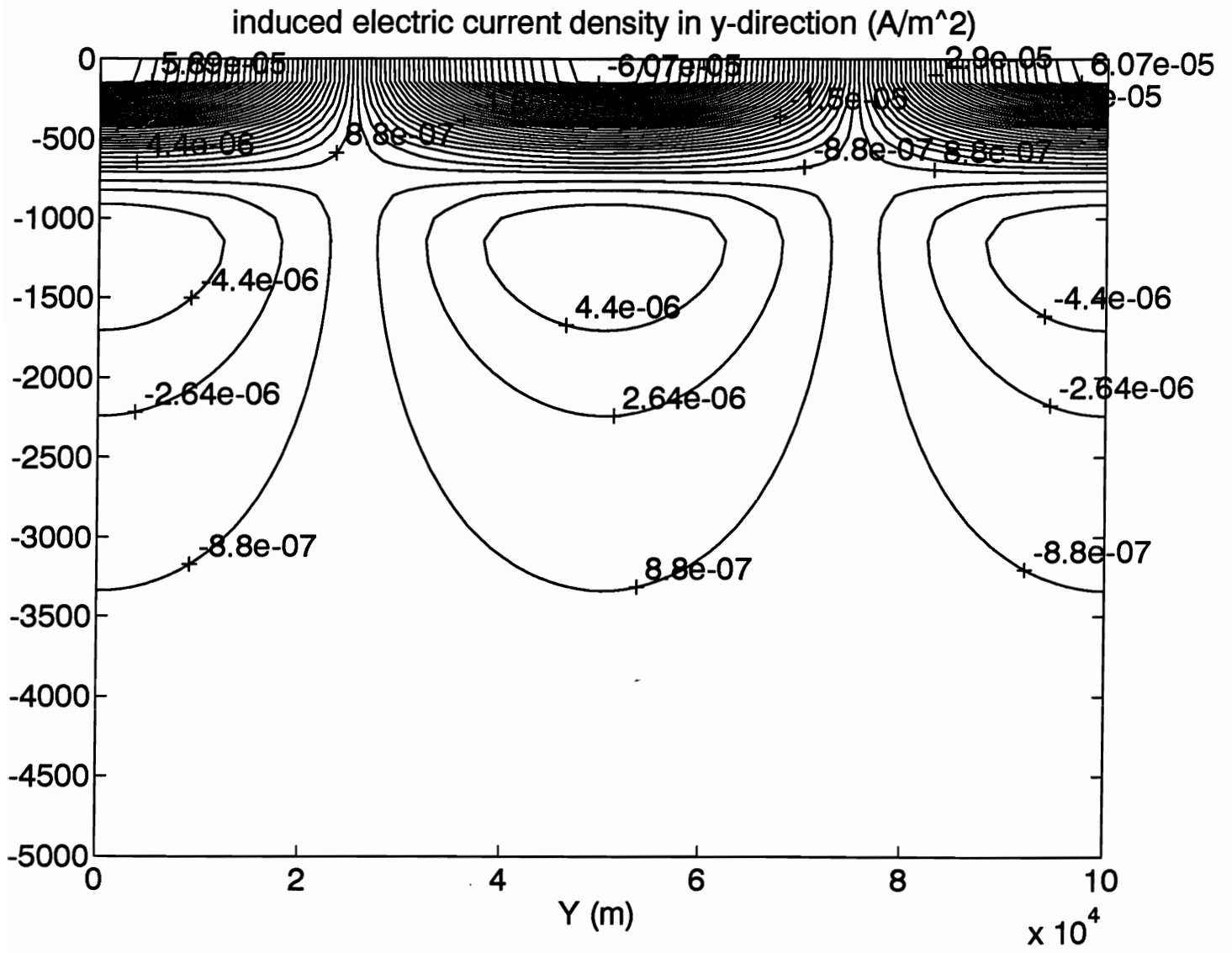


Figure 7 (c)

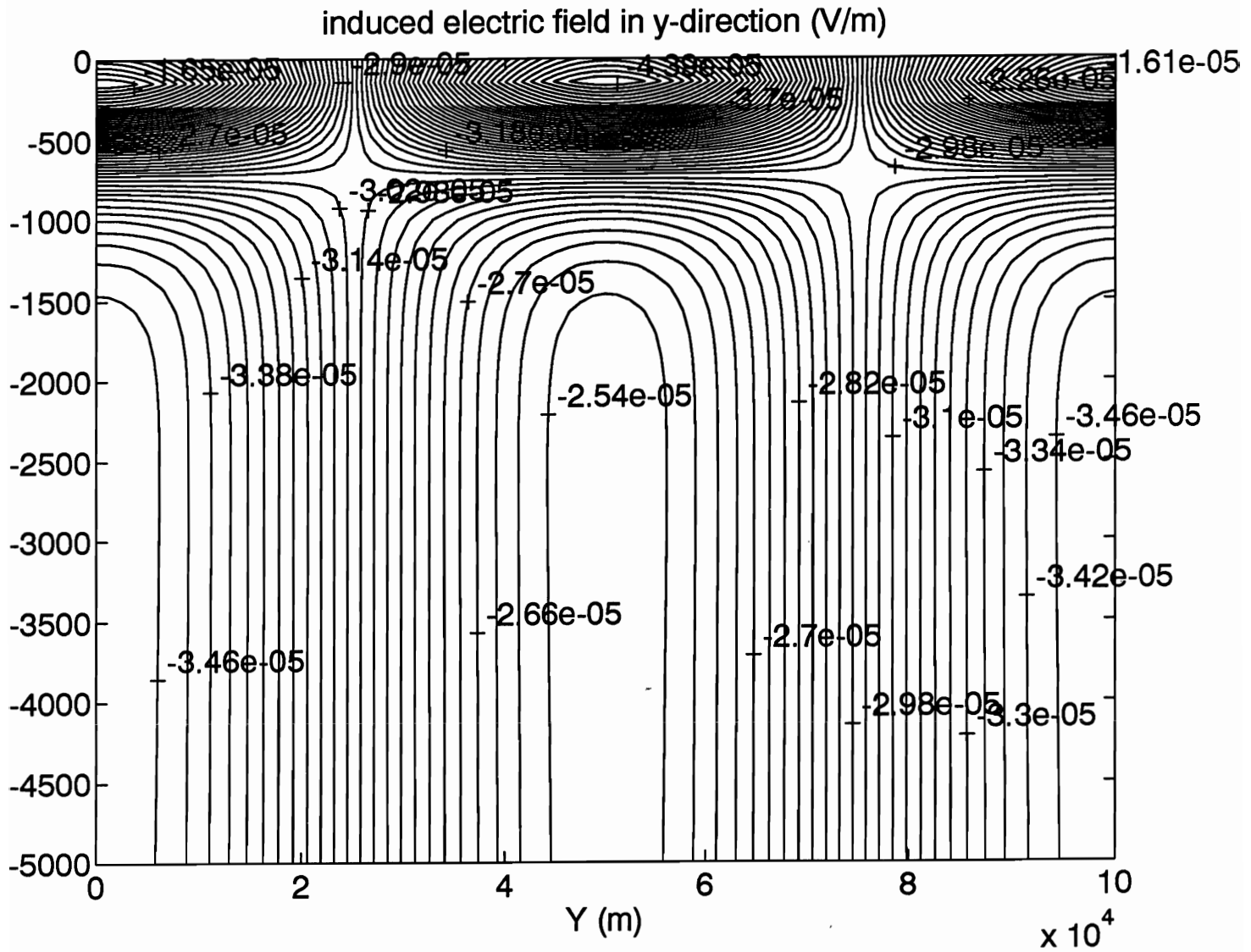


Figure 7 (d)

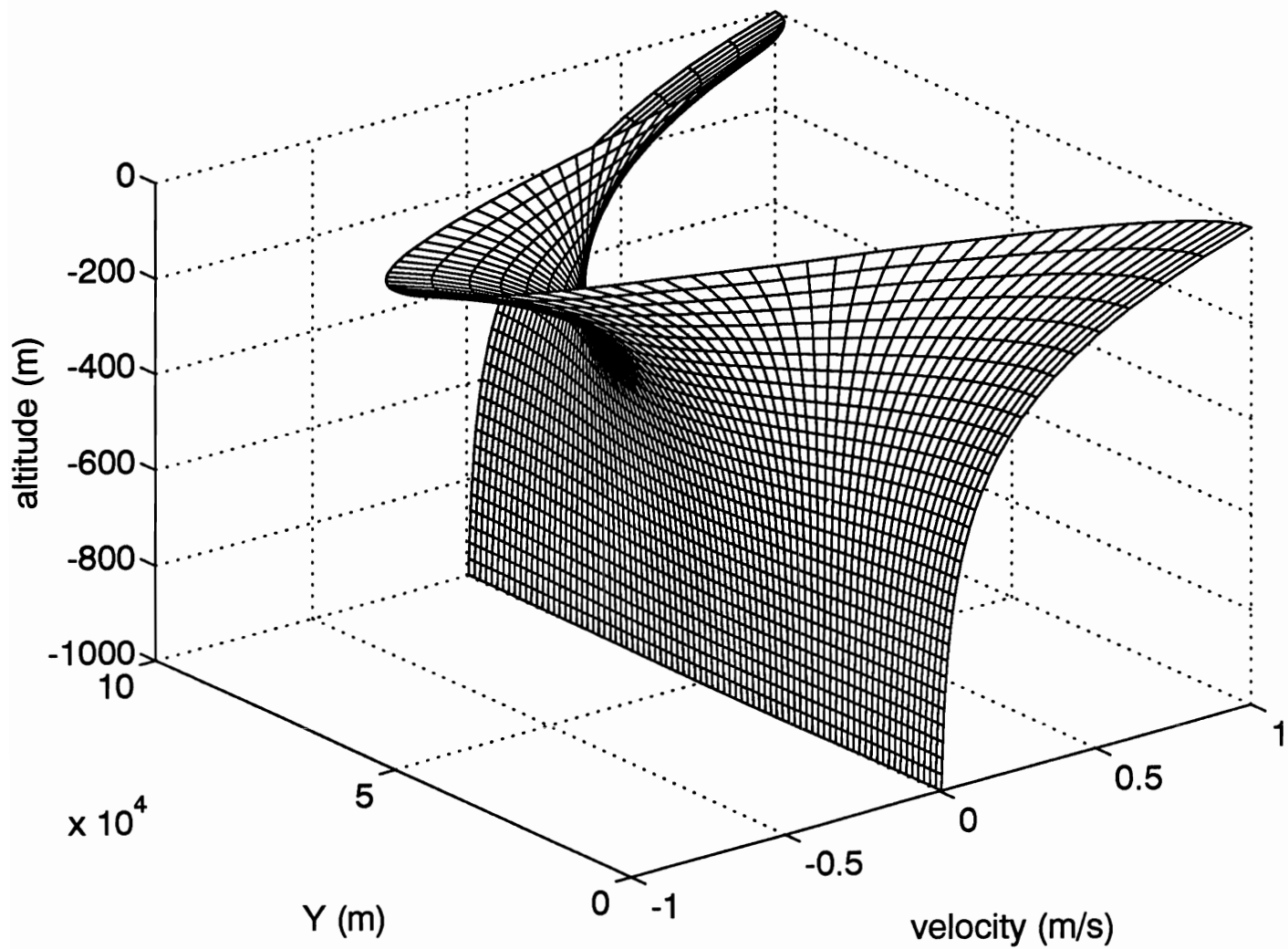


Figure 8 (a)

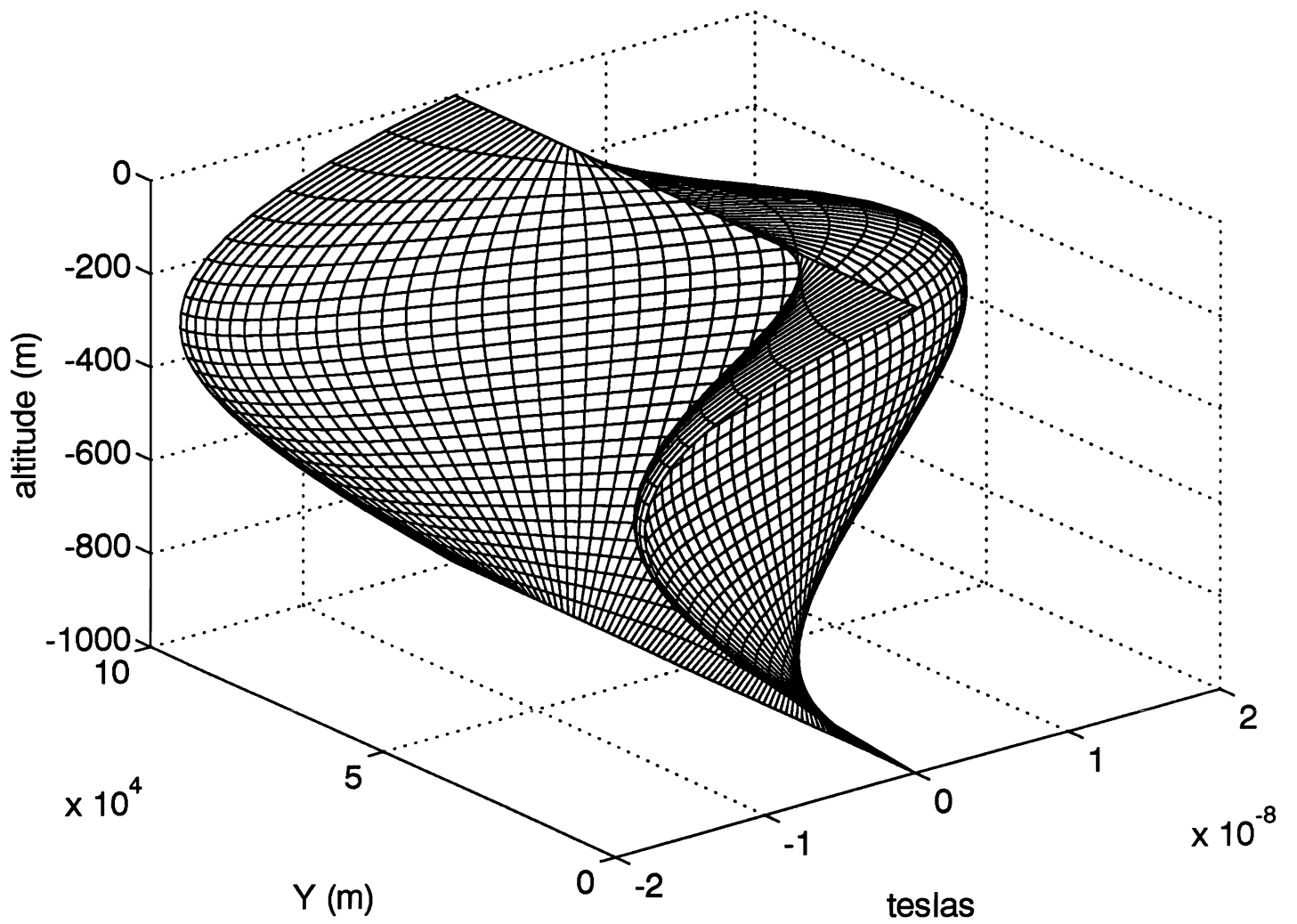


Figure 8 (b)

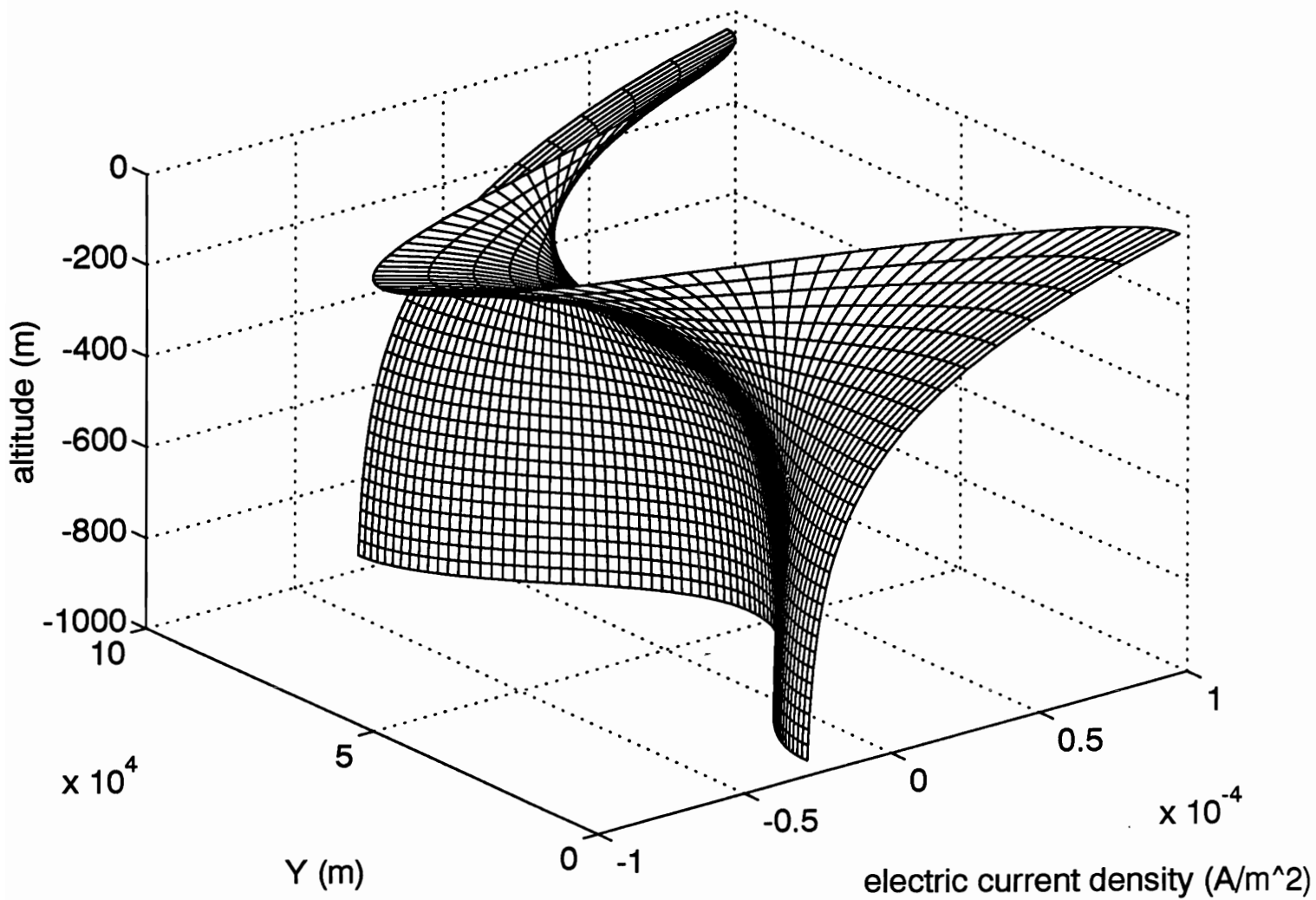


Figure 8 (c)

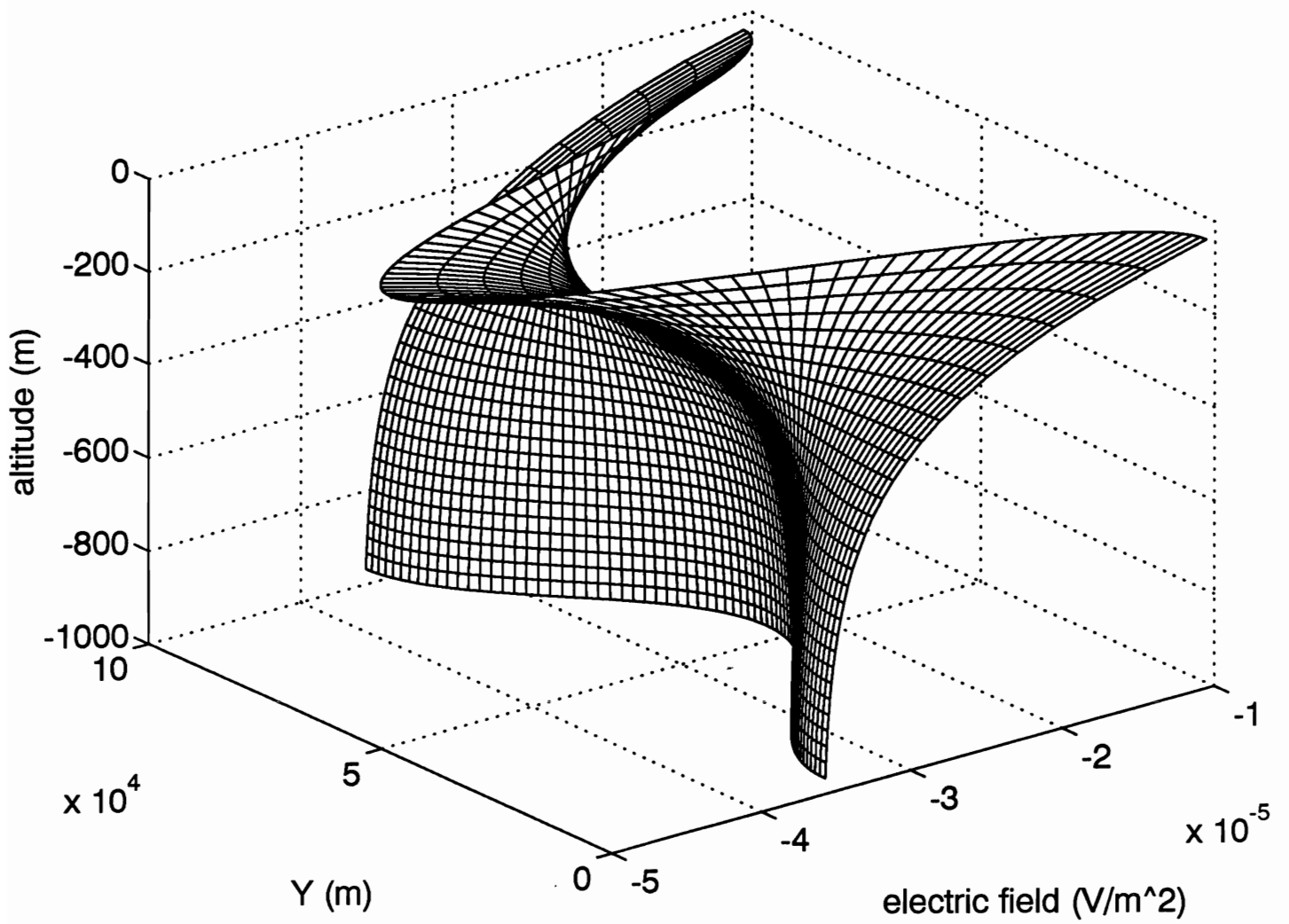


Figure 8 (d)

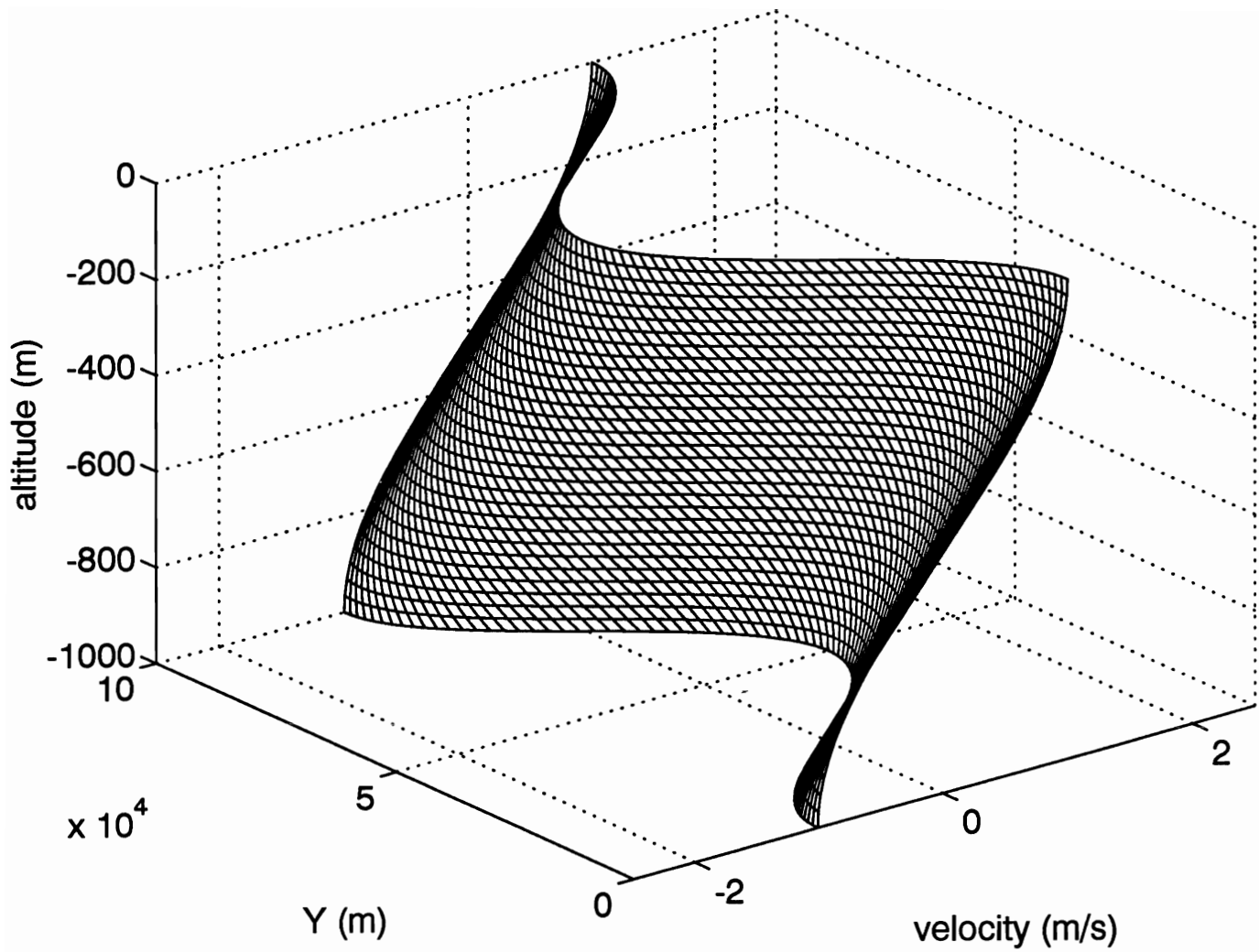


Figure 9 (a)

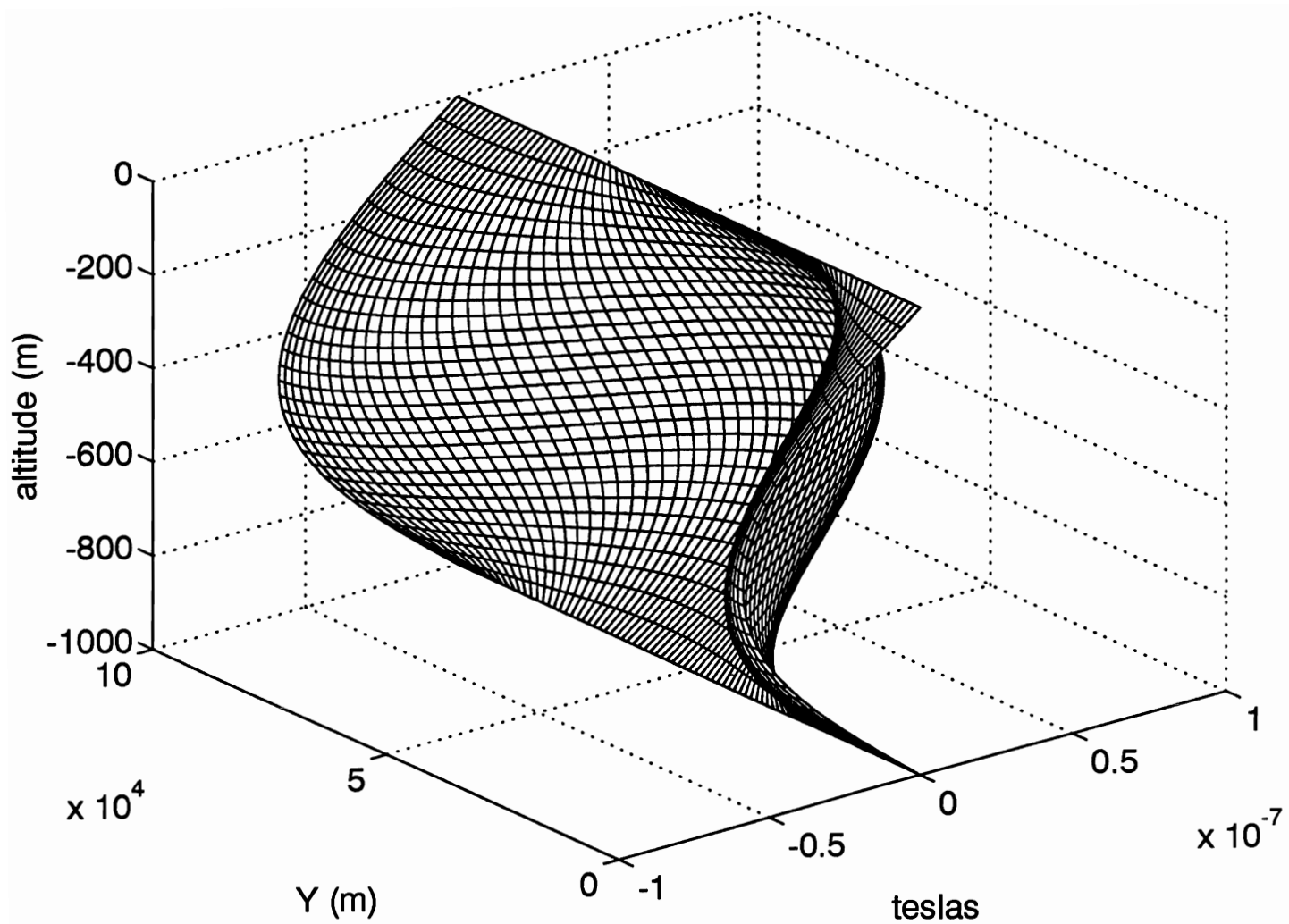


Figure 9 (b)

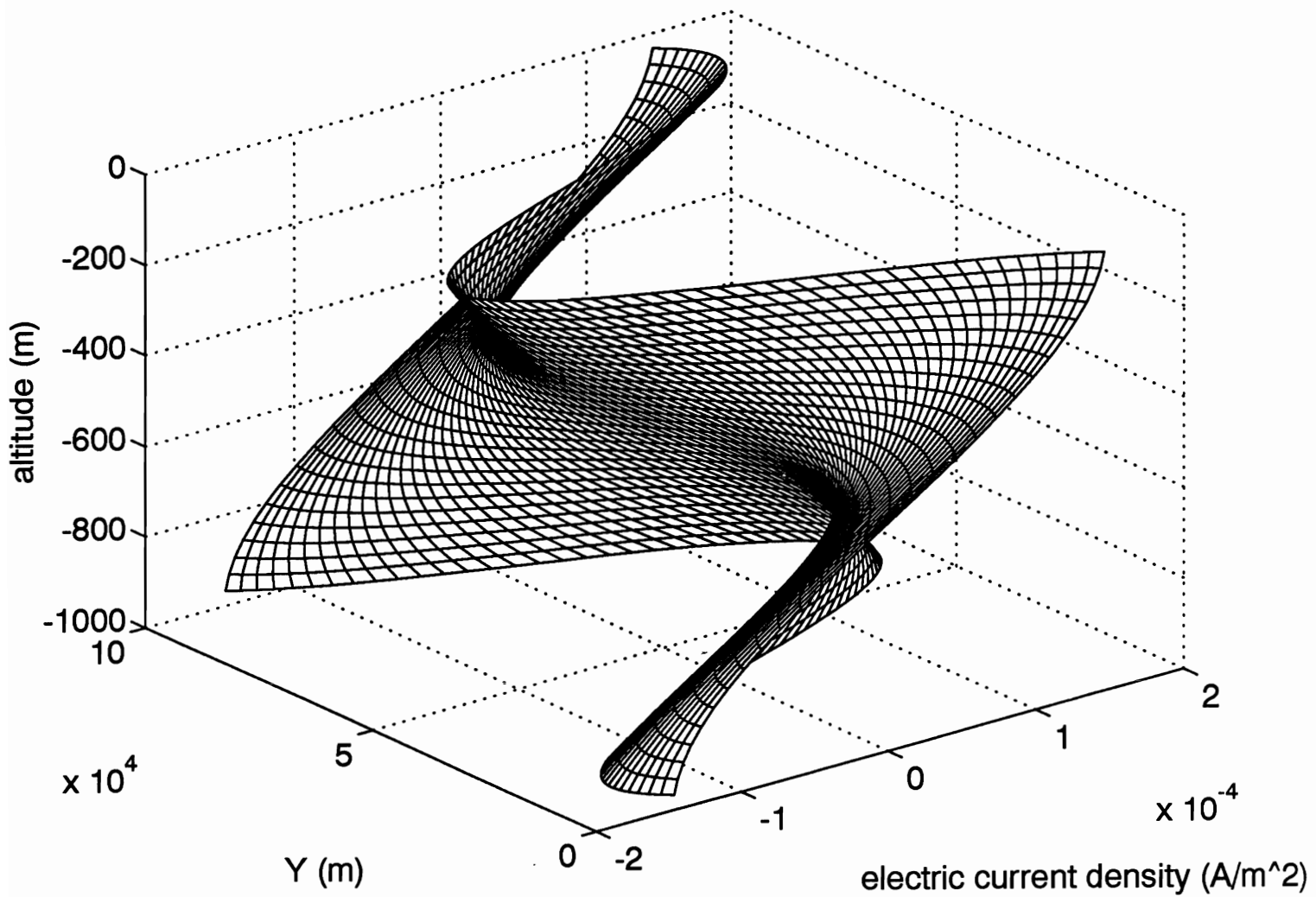


Figure 9 (c)

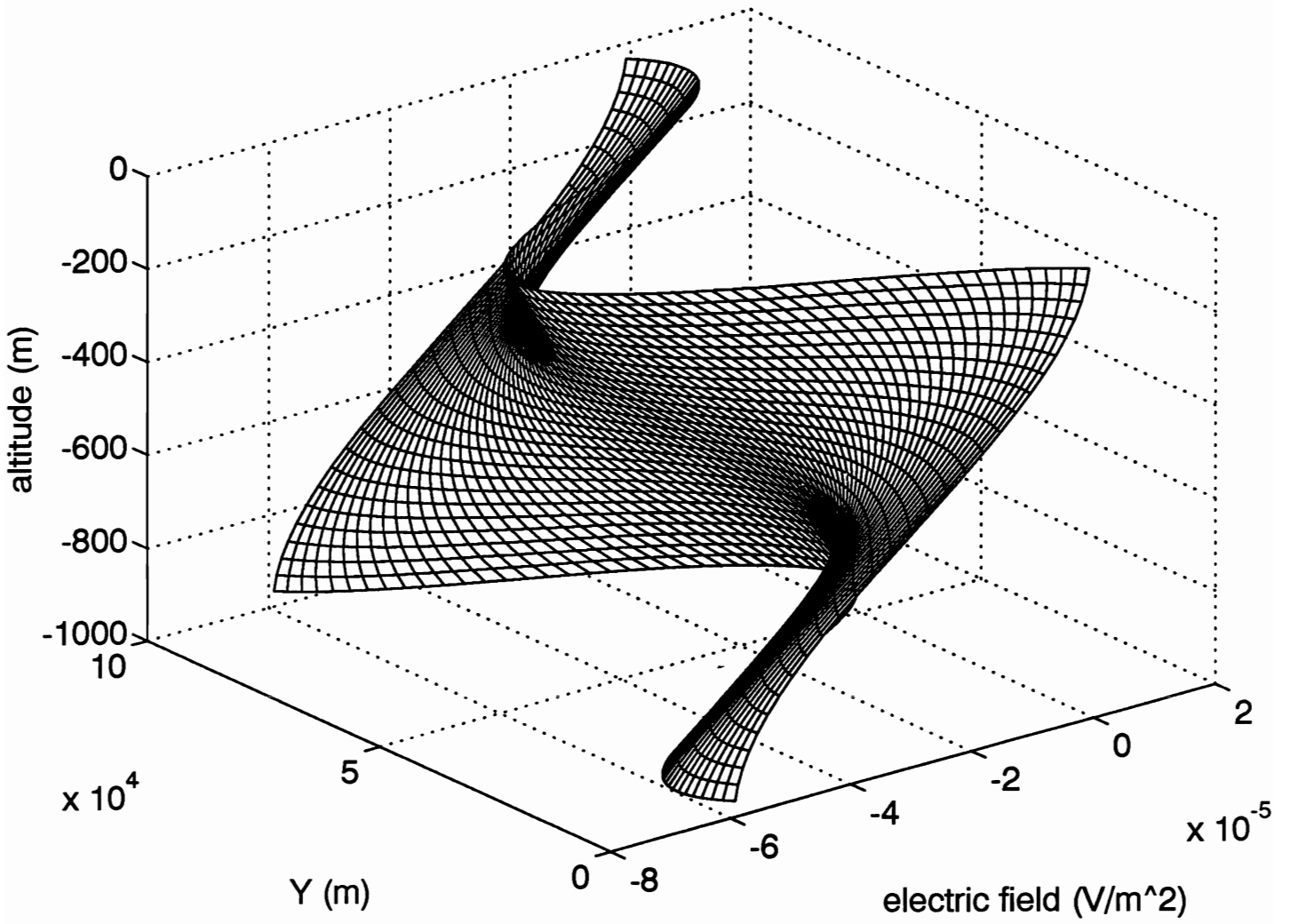


Figure 9 (d)

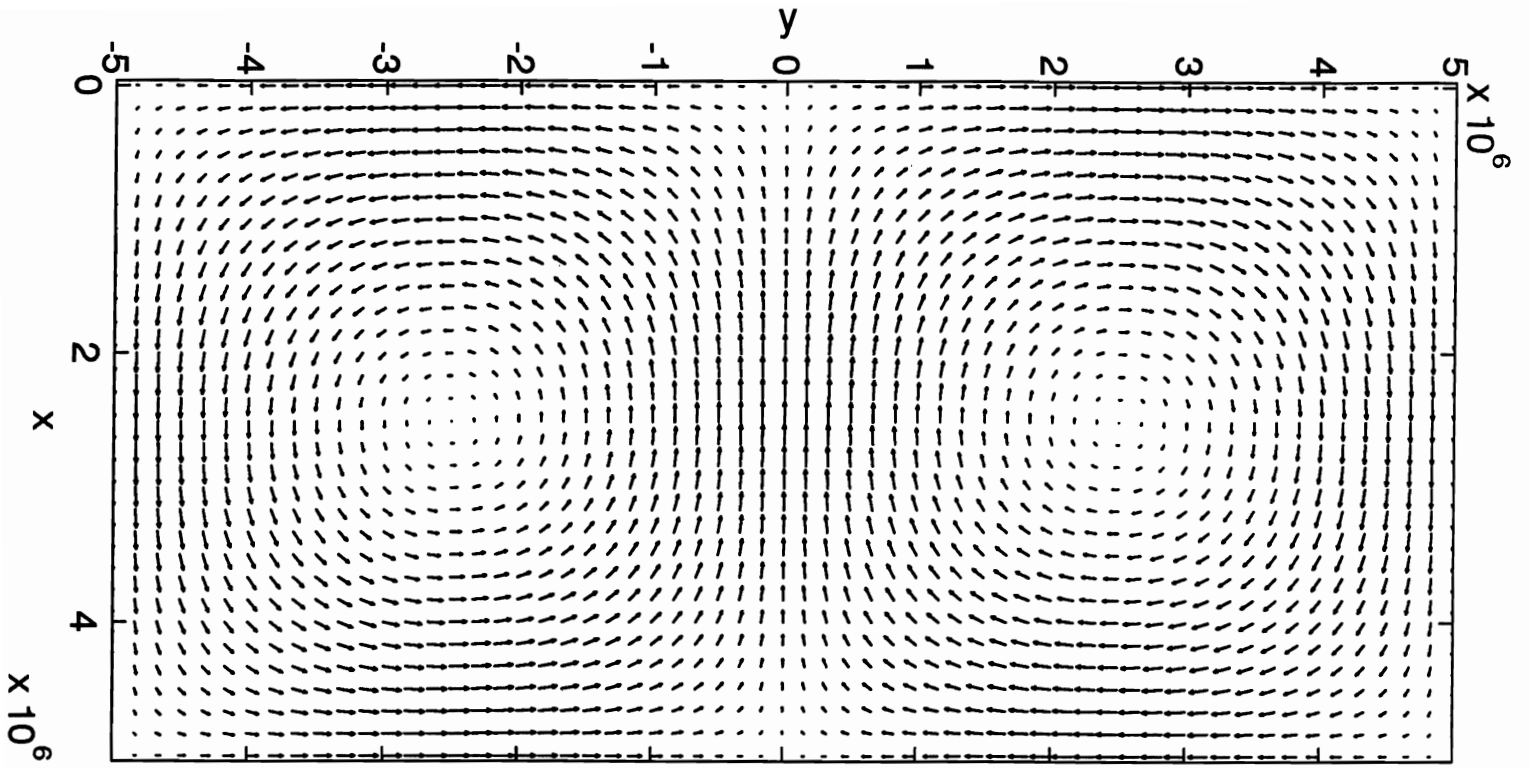


Figure 10

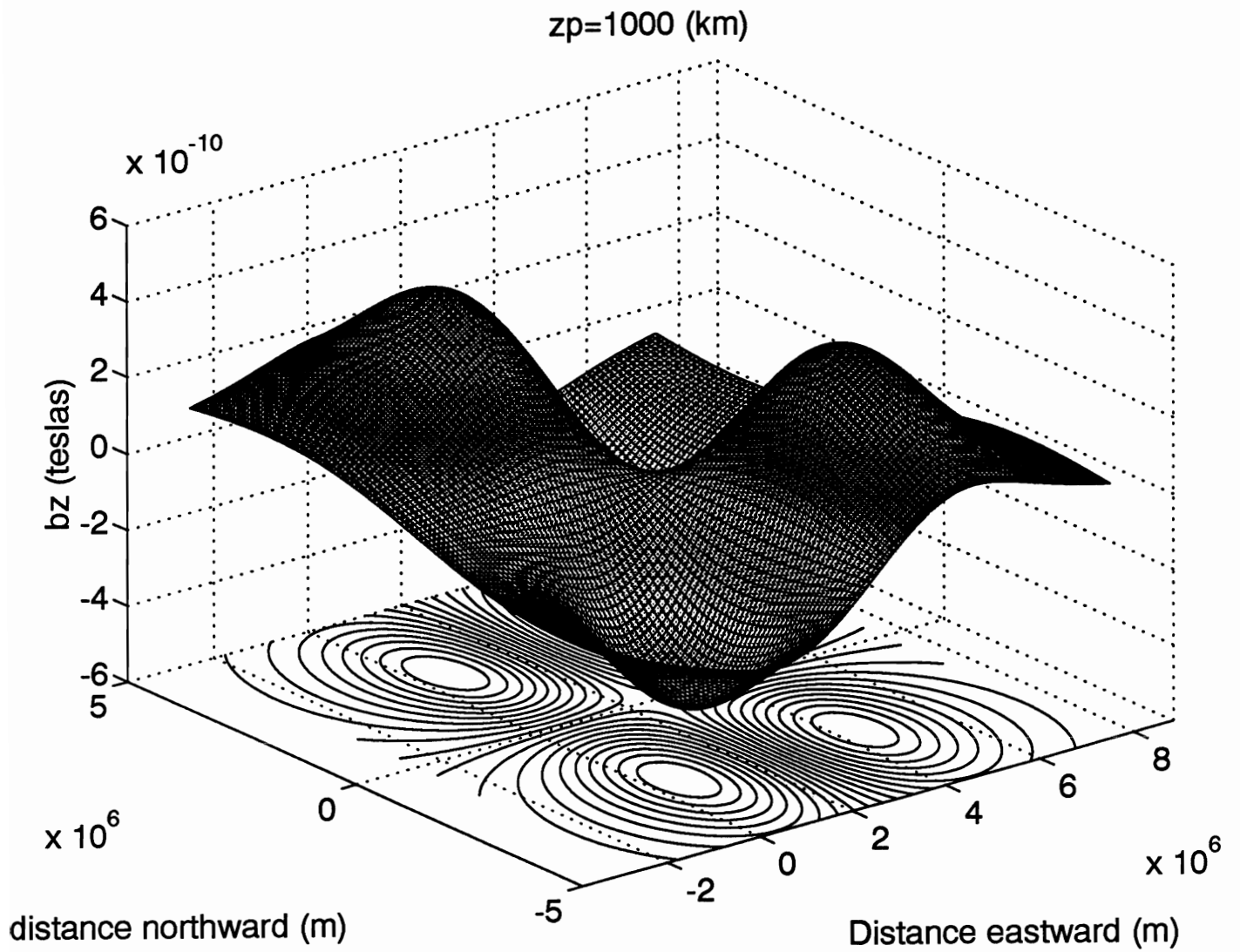


Figure 11

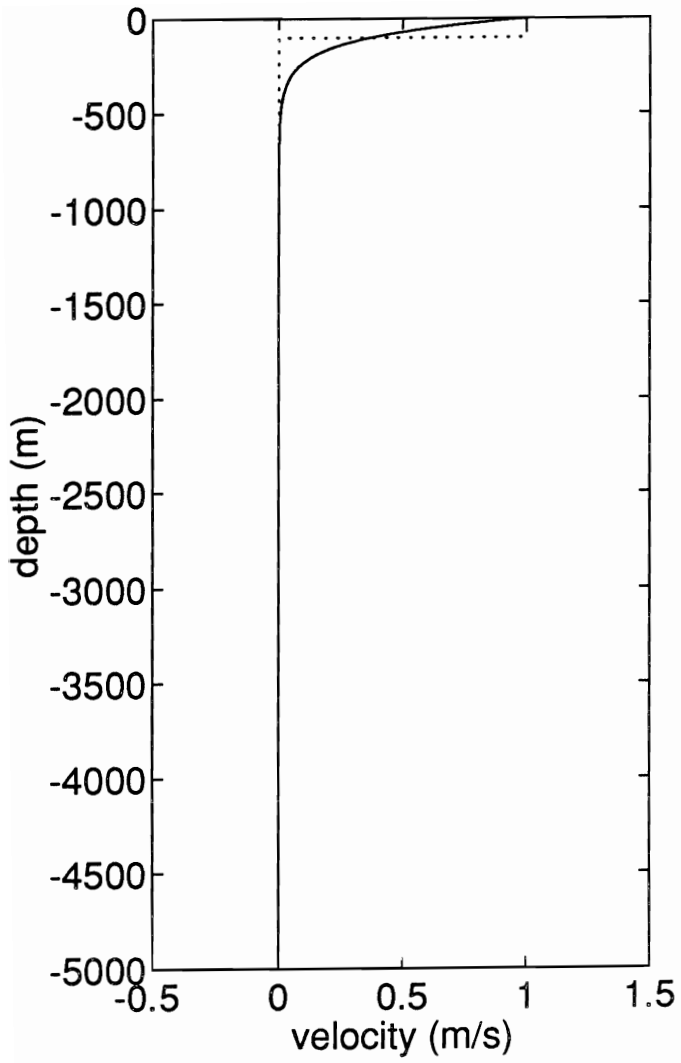


Figure 12 (a)

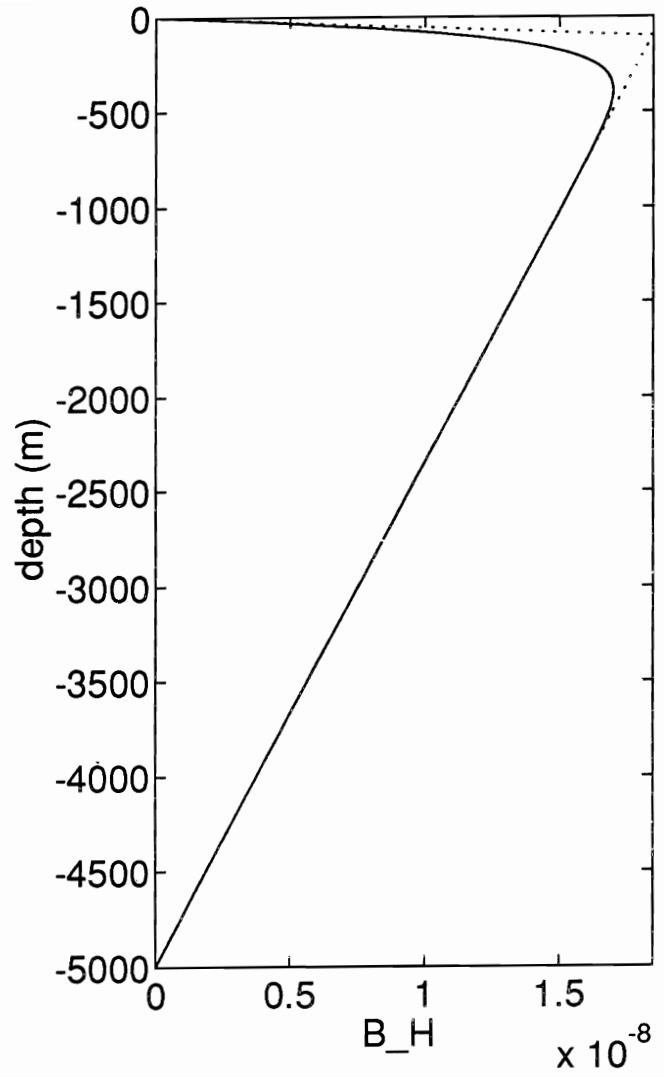


Figure 12 (b)

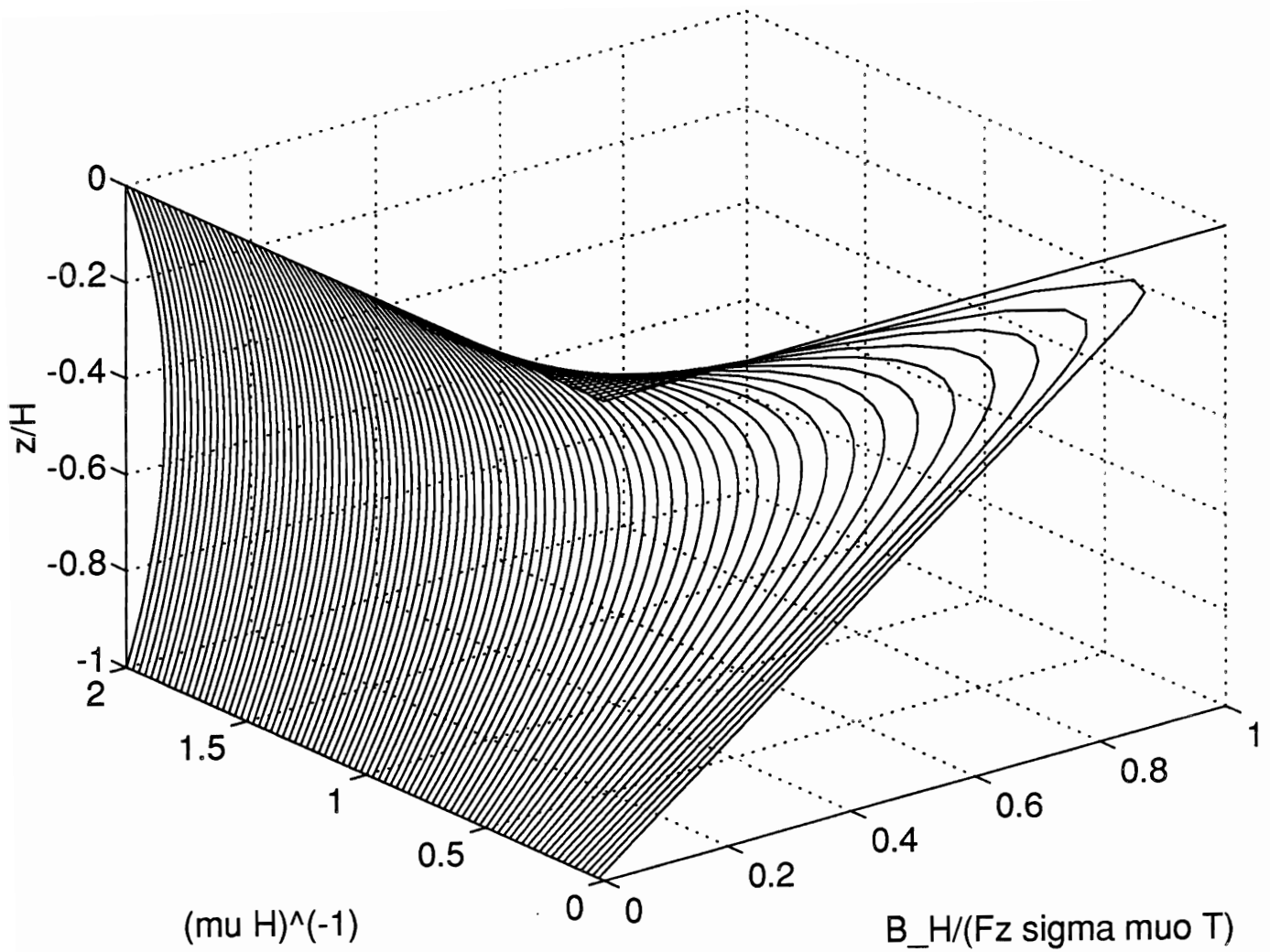


Figure 13

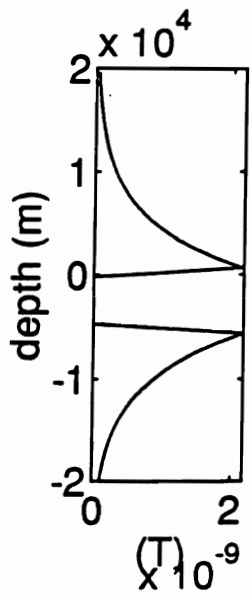
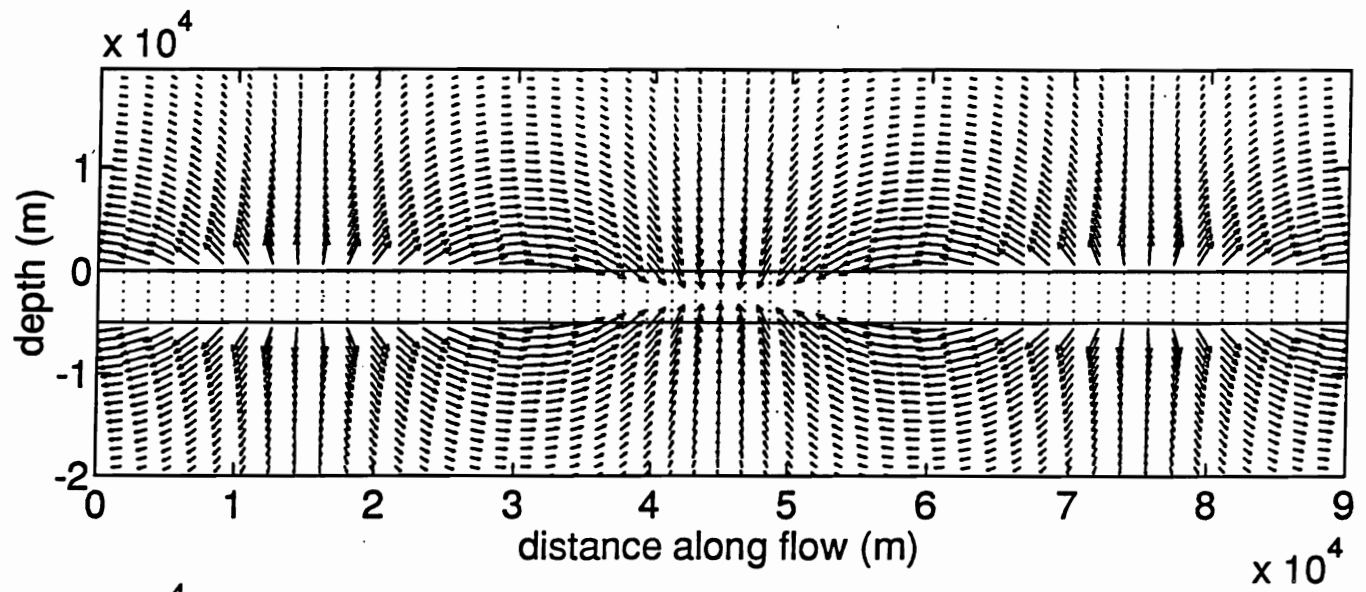


Figure 14 (a)

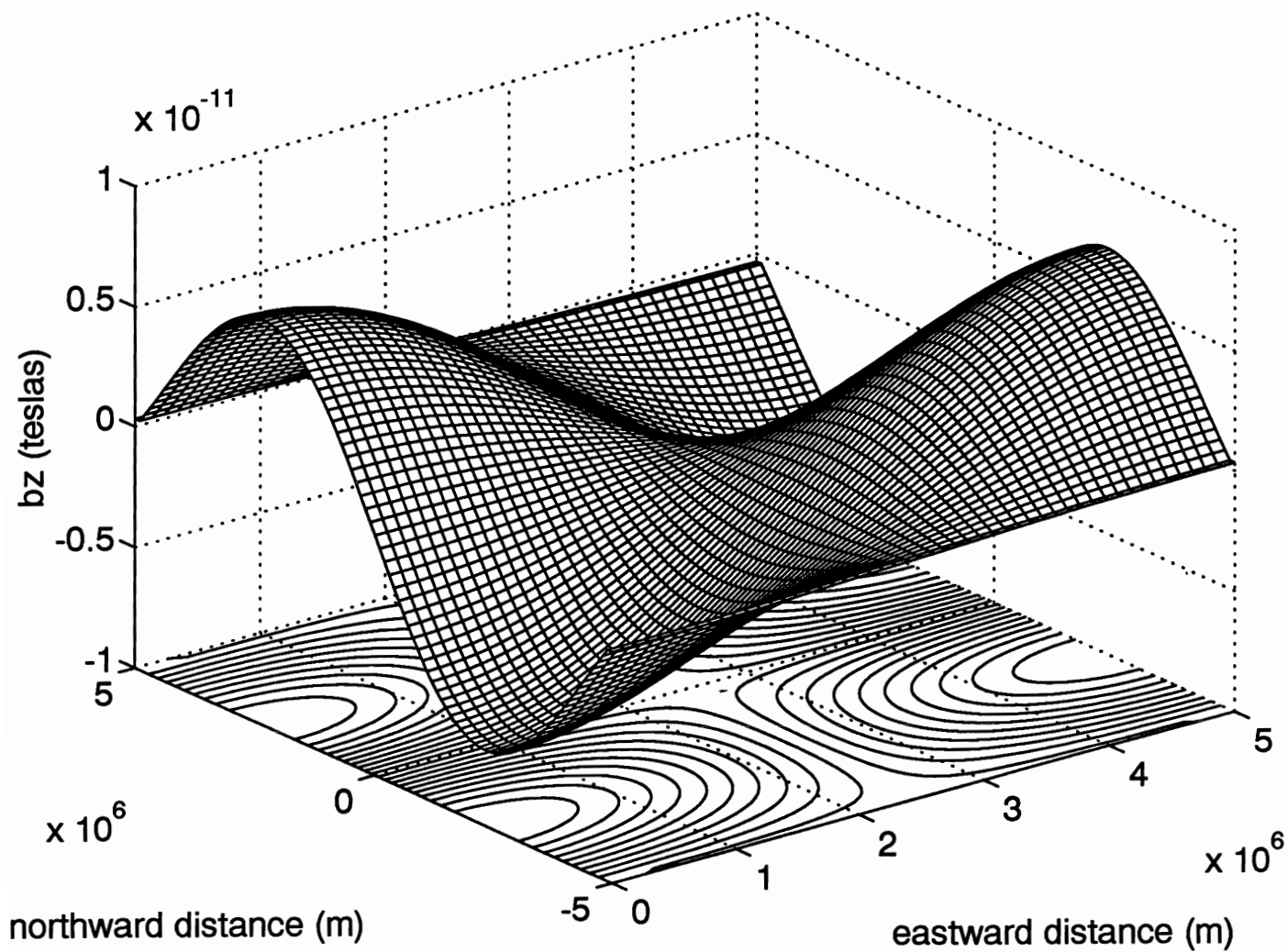


Figure 14 (b)